UNIVERSITÀ DEGLI STUDI
DI MODENA E REGGIO EMILIA

Dottorato di ricerca in Molecular and Regenerative Medicine

Ciclo XXXII

PRECLINICAL ASSESSMENT OF AN ATMP FOR SEVERE HYPOSPADIAS TREATMENT

Candidato: Matteo Melonari

Relatore: Prof. Graziella Pellegrini

Coordinatore del Corso di Dottorato: Prof. Michele De Luca

CONTENTS

ABSTRACT

Preclinical assessment of an ATMP for severe hypospadias treatment

Urethral reconstruction has received growing attention in recent years due to pathologies such as hypospadias, a very common congenital male genitalia malformation with a European prevalence of around 18.6 new cases per 10,000 births, and a very high urethral stricture recurrence rate after treatment. Unfortunately, the current care standard to repair hypospadias expects a high long-term complication rate requiring repeated surgery in approximately half of the patients. Various surgical techniques have been developed to obtain the best risk-to-benefit ratio, and one of them operates using a split-thickness autologous oral mucosa grafts for urethral plate substitution. However, this procedure adds other complications at donor site such as pain, persistent difficulty in mouth opening, and infections. Tissue engineering and epithelial stem cell culture can further improve hypospadias surgery, reducing invasiveness and morbidity, and overcoming issues such as customizable graft size lack and only two tissue withdrawal chances. Indeed, large tissue amounts can be obtained from few stem cells deriving from a small biopsy for damaged or lost tissue repair and regeneration, supporting wound healing, limiting inflammatory reactions, and decreasing post-operative complications. Therefore, this study explores the feasibility of a new advanced therapy medicinal product (ATMP) aimed at tissue engineering for severe hypospadias patient's urethra reconstruction. The ATMP would consist of *ex vivo* expanded autologous human oral mucosa epithelial keratinocytes containing stem cells grown on a biocompatible fibrin scaffold. Urethral and oral mucosa keratinocytes cultures were performed under Good Manufacturing Practice (GMP). Cell and tissue characterization and evaluation were aimed at determining whether oral mucosa epithelia could work as a substitute for urethra engineering after *in vitro* culturing and expansion. The long-term regenerative properties of both tissues were confirmed, and single-clone assays were performed to analyze epithelial stem cell content, and gene expression profiles. Comparison of the two epithelia revealed the same high proliferative potential for urethra and oral mucosa cultures. Marker expression was very similar, although maintenance of specific markers occurred. Clonal analysis did not highlight a significantly different stem cell proportion. Preclinical experiments were accomplished to assess ATMP identity, purity, and potency. Therefore, thanks to cells selected

by means of epithelial stem cell markers, and ATMP regenerative potency and purity evaluations, the resulting cultured tissue can engraft, persist, and self-renew over time. Finally, fibrosis-derived urethral stenosis is one of the main complications after primary hypospadias treatment, therefore, the inflammatory profile of patients was investigated to predict the stricture susceptibility. Urinary proteomes have been examined to distinguish patients likely to develop inflammatory-related complications. In the long run, the analysis of those biomarkers could be predictive of the clinical success and can aid at a well-defined patient selection for therapy improvement.

SINTESI

Studio preclinico di un ATMP per il trattamento di gravi forme d'ipospadia

Recentemente la ricostruzione uretrale ha ricevuto attenzioni sempre più crescenti a causa di patologie come l'ipospadia, una malformazione dei genitali maschili molto comune, con una prevalenza europea di circa 18,6 casi ogni 10.000 nati ed un alto tasso di stenosi uretrali dovuti a terapie fallimentari. Purtroppo, le attuali procedure chirurgiche prevedono complicazioni molto frequenti dopo il trattamento e circa metà dei pazienti hanno bisogno di un secondo intervento. Varie tecniche chirurgiche sono state sviluppate per cercare di ottenere il miglior rapporto rischio-beneficio. Una di queste utilizza un innesto di mucosa orale a spessore parziale per la ricostruzione del lume uretrale, portando però altre complicazioni al sito di prelievo, come dolore, difficoltà persistente nell'aprire la bocca ed infezioni. L'ingegneria tissutale e le colture di cellule staminali epiteliali possono migliorare la chirurgia dell'ipospadia, riducendo l'invasività e risolvendo problemi come l'impossibilità di scegliere la dimensione dell'innesto ed avere soltanto due possibilità di prelievo della mucosa orale. Infatti, grandi quantità di tessuto possono essere prodotte a partire da poche cellule staminali derivanti da una piccola biopsia per la rigenerazione di un tessuto perso o danneggiato, supportando la guarigione della ferita, limitando reazioni infiammatorie e diminuendo complicazioni post-operatorie. Perciò questo studio esplora la possibilità di sviluppare un nuovo prodotto medicinale di terapia avanzata (ATMP) finalizzato all'ingegneria tissutale dell'uretra per pazienti affetti da gravi forme d'ipospadia. L'ATMP consisterebbe di cheratinociti autologhi di mucosa orale umana espansi *ex vivo* e coltivati su un supporto biodegradabile di fibrina. Le colture di cheratinociti uretrali e buccali sono state eseguite seguendo le norme vigenti di buona fabbricazione (GMP). Le caratterizzazioni cellulare e tissutale sono state compiute per determinare se l'epitelio della mucosa orale potrebbe funzionare come sostituto per l'ingegnerizzazione dell'uretra dopo la coltura e l'espansione *in vitro*. Le proprietà rigenerative a lungo termine di entrambi i tessuti sono state confermate e saggi su singoli cloni sono stati eseguiti per analizzare il contenuto di cellule staminali epiteliali ed i profili di espressione genica. I confronti di entrambi gli epiteli hanno rivelato lo stesso alto potenziale proliferativo. L'espressione dei marcatori è stata analoga, pur mantenendo l'espressione di marcatori specifici. Le analisi clonali non hanno sottolineato differenti

proporzioni del compartimento staminale. Esami preclinici sono stati eseguiti per determinare l'identità, la purezza e la potenza dell'ATMP. Grazie alla selezione di cellule mediante marcatori staminali epiteliali, le valutazioni della potenza rigenerativa e della purezza dell'ATMP, il risultante tessuto coltivato può attecchire, persistere nel sito e autorigenerarsi. Infine, le stenosi uretrali derivanti da fibrosi sono una delle maggiori complicazioni dopo il trattamento dell'ipospadia, perciò il profilo infiammatorio di pazienti è stato investigato per predire la tendenza allo sviluppo di stenosi. I proteomi urinari sono stati esaminati per distinguere pazienti con possibilità di sviluppare complicazioni correlate allo stato infiammatorio. In futuro, le analisi di specifici biomarcatori potrebbero essere predittive del successo clinico e favorire una migliore selezione dei pazienti per il perfezionamento della terapia.

1. INTRODUCTION

1.1. Hypospadias

External genitalia birth defects are one of the most common congenital anomalies in humans. Hypospadias is a condition of the urethra where the urethral meatus is not at the usual location on the glans (Baskin *et al.*, 2006). The most frequently adopted disease classification is based on urethral meatus location, as it may be in several different positions between the glans and the perineum. Thus, the disease is classified as distal, medial, and proximal (Fig.1.1). The meatus is found in the distal position near the penis end in 70% of the cases, but it may also be found at the proximal position at the base of the penis in 20% of the cases, and in the middle of the penile shaft in 10% of the cases (van der Zanden *et al.*, 2012). The urethral meatus misplacing is caused by urethral corpus spongiosum and ventral prepuce abortive developments, with a consequent impairment in the normal urethral embryological development (Baskin *et al.*, 2006). Although urethral meatus location is important, other anatomical variables are to be evaluated to assess disease severity, such as glans configuration and type of curvature (Manzoni *et al.*, 2004). In 15% of the distal cases the penis curves downward, a condition called chordee. Penile shortening and ventral chordee are, however, more likely to occur with the most serious proximal defects: in fact, when the meatus opens further down the shaft, chordee occurs in more than 50% of patients (Mouriquand & Mure, 2001). Moreover, the urinary meatus may be narrowed, a condition called meatal stenosis. Hypospadias causes urination and ejaculation complications, since the penis curvature may cause painful erections, and difficult penetration and can make it complicated to perform sexual activities. Therefore, patients can develop psychological problems, affecting social life and triggering anxiety or depression in some cases (Manzoni *et al.*, 2004). Pathological incidence has been increasing in the past decades (Paulozzi *et al.*, 1997), and hypospadias prevalence in Europe is around 18.6 new cases per 10,000 births (Bergman *et al.*, 2015). However, there is a considerable variation from country to country (Kallen *et al.*, 1986). Hypospadias is generally more common among monozygotic twins and hypospadias patient male children, which prevalence is 8% (Gatti *et al.*, 2003).

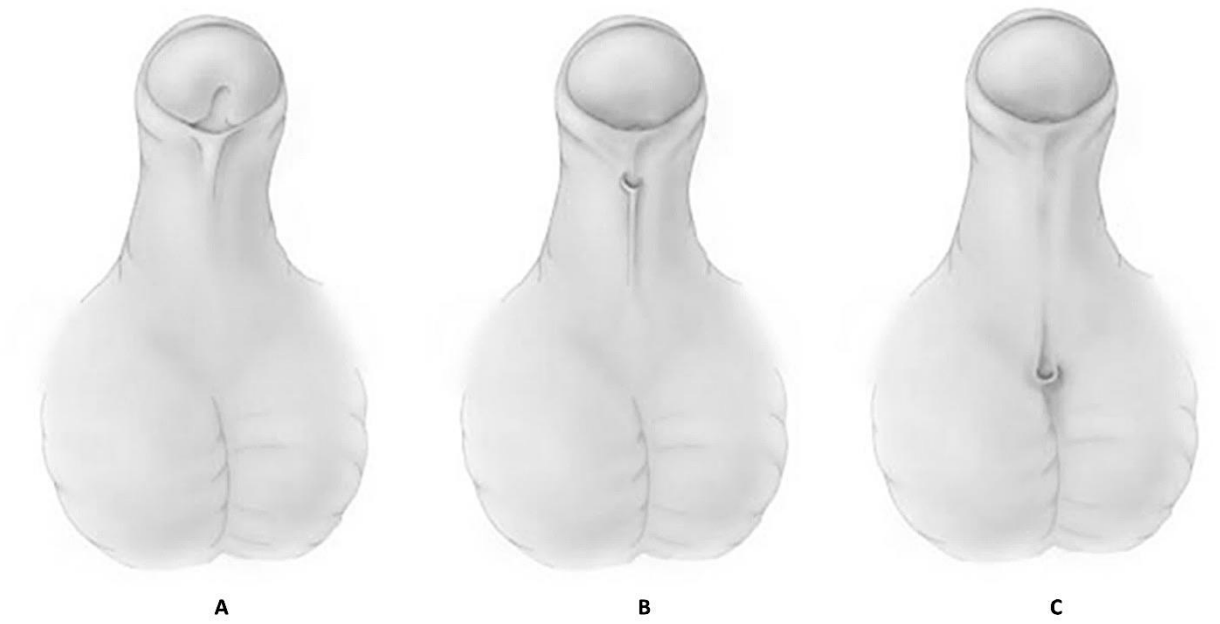

Figure 1.1. ***Hypospadias classification. (A) Subcoronal. (B) Midshaft. (C). Penoscrotal.*** *Severity degrees depend on urethral meatus location, but also other anatomical variables concur in determining the disease severity.*

1.2. Treatment

Hypospadias repair treatment is aimed to make the patients urinate correctly, have sexual intercourse, and to present an acceptable cosmetic appearance. To these accounts, surgeons' efforts address the penis straightening by orthoplastic chordee correction, the urethral meatus placement at the glandular location by urethroplasty and meatoplasty, and glans reconstruction by glansplasty, to obtain functional, sexual and esthetic successes (Culp & McRoberts, 1968). Currently, most surgeons claim that primary hypospadias repair ideal time is the age of 6-12 months. The main reason being that genitals awareness allow an improved emotional and psychological result (Manzoni *et al.*, 2004). The more common surgical interventions involve the one-stage Snodgrass (Snodgrass, 1994; Fig.1.2) or the two-stage Bracka techniques in the first year of life (Manzoni *et al.*, 2004; Fig.1.3). Hypospadias correction surgeries often involve urethral plate substitution employing skin flap or oral mucosa. Skin flap use infers a one-chance only to use foreskin and in the case of first-surgery failure, a flap of skin taken from a different site could cause hair growth or infections development. Moreover, skin use implies scar presence at the withdrawal site. From a histological perspective, skin epithelium develops an envelope in contrast with its absence in the wild-type urethral epithelium. Due to these side effects, the

majority of urethroplasty surgeries employs oral mucosal grafts. Oral mucosa has a high strength and regenerative capacity to react to daily damages due to chewing. It is an easily accessible tissue, since the withdrawal is done at the inner cheek. Moreover, oral mucosa epithelium is widely used in pharyngeal and maxillofacial surgeries (Yarington, 1980), reconstructive vaginal defect procedures (Grimsby & Baker, 2014), and for urethroplasty.

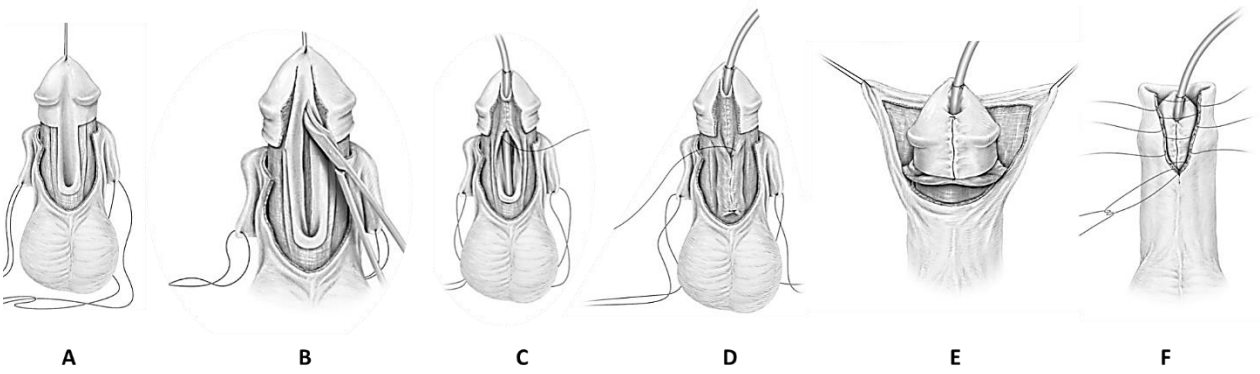

Figure 1.2. ***Snodgrass technique main steps. (A) Initial skin incision.*** *After degloving, the corpus spongiosum alongside the urethral plate is dissected off the underlying corpora cavernosa.* ***(B) Midline incision.*** *Urethral plate penile aspect midline incision is made to assess tissue health. Glans wings are next dissected from the urethral plate.* ***(C) Tubularization.*** *The urethral plate is tubularized beginning at the neomeatus. Tubularization is completed turning all epithelium into the neourethral lumen.* ***(D)*** *The previously mobilized corpus spongiosum is closed, followed by repair coverage by a dartos pedicle flap.* ***(E) Glansplasty****.* ***(F) Skin closures*** *(Snodgrass, 2005; illustrations by Stephan Spitzer, www.spitzer-illustration.com)*

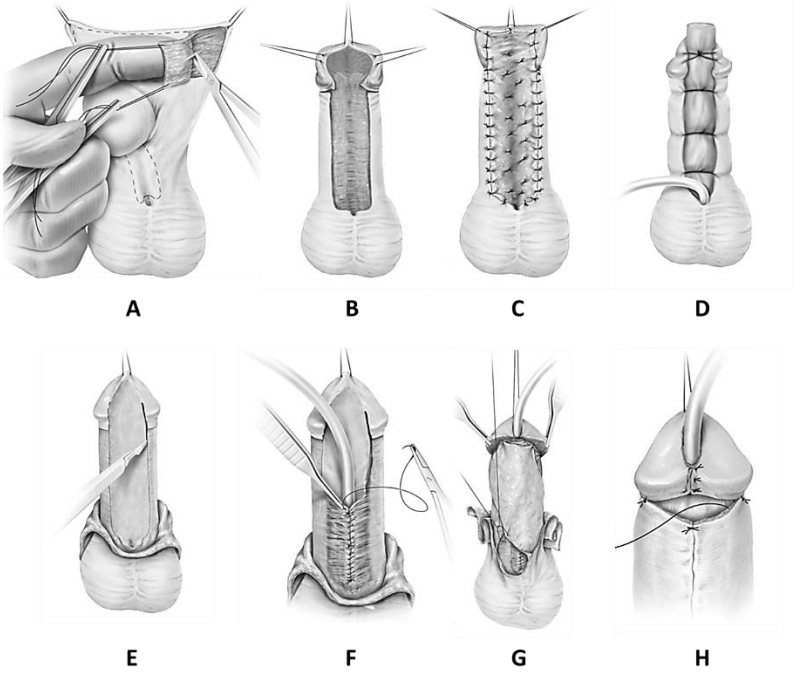

Figure 1.3. ***Bracka technique main steps. (A)*** *The incision is made at the marked preputial skin strip side. The graft is then dissected by applying counter pressure with the finger while holding the stay sutures.* ***(B) Glans wings dissection.*** *The urethral plate is excised.* ***(C) Graft quilting.*** *The graft is quilted in the midline to demarcate the glans cleft, and to the* corpora *at regular intervals to stabilize the graft on the wound bed.* ***(D)*** *The lateral glans stay sutures are now tied over a nonadherent bolus dressing.* ***(E)*** *The penis is degloved at the Buck's fascia level.* ***(F)*** *The neourethral plate is tubularized.* ***(G)*** *A protective dartos fascia flap is placed over the entire suture line as a waterproofing layer.* ***(H)*** *The glans spongiosum is reconstructed completing the glans wings medial rotation and closure below the meatus (Altarac* et al.*, 2012; illustrations by Stephan Spitzer, www.spitzer-illustration.com).*

1.2.1. Complications

Oral mucosa epithelium use in current surgery implies some complications. Patients reports pain, difficulty in mouth opening, and changes in salivary function with a morbidity rate of 3-4% at the donor site (Markiewicz *et al.*, 2008). Also, scars and oral contractures are present in about 20% of cases (Fasolis *et al*., 2014). Mechanical irritation from oral mucosa dental rubbing and parafunctional biting is associated with oral cancer development (Perry *et al.*, 2015). Moreover, since full thickness withdrawal is invasive, it only allows two removal chances. Several complications were also described at the recipient site, such as graft adherence lack, urethral strictures, and graft contractures responsible for penis curvature. Therefore, oral mucosal application for urethra reconstruction in hypospadias patients does not represent a long-term and conclusive solution. As a matter of fact, about 60% of patients undergoing urethra reconstruction by oral mucosal graft requires two surgical steps to resolve residual complications, and 39% of the patients requires more than two surgical steps before achieving satisfactory results (Barbagli *et al.*, 2006).

1.3. Strictures

Hence, regardless the increasing hypospadias surgery frequency and notwithstanding surgical technique advances, complications following hypospadias repair treatment remains one of the most challenging problems faced by pediatric urologists. Among the failed hypospadias treatment patients, 37% have one complication, while 43% have two complications including urethral strictures for 56.6% of the cases, residual hypospadias for 43.3%, and meatal stenosis for 18.3% (Barbagli *et al.*, 2006). Urethral stricture is a scarring process of the urethral mucosa and the surrounding spongy tissue (Huang *et al.*, 2018). It might occur in the meatal region, or along the anastomosis between the native urethra and the neourethra (Gürdal *et al.*, 2004). Strictures at surgery site may be apparent either shortly after the surgery, or until adolescent or early adult life (Tang *et al.*, 2008). Hypospadias repair may also fail many years after achieving successful functional results, with subsequent urethral stricture development decades after initial hypospadias surgery (Uemura *et al.*, 2000). Moreover, treatment for complications remains complex because the penis is usually densely scarred, inflamed and significantly shortened from prior surgeries (Barbagli *et al.*, 2006). Urethral stricture clinical diagnosis is generally based on

retrograde and voiding cystourethrographies, and cystoscopy. They also determine stricture location, degree, and extension (Andersson *et al.*, 2011). Various surgical options such as urethral dilation, internal urethrotomy, and urethroplasty are used to manage urethral stricture disease (USD). However, these procedures have a high failure rate and poor long-term outcome for patients (Hampson *et al.*, 2014). Although urethroplasty represents the standard treatment for urethral stricture, it is an invasive procedure that is associated with complications such as erectile dysfunction (Fossati *et al.*, 2016). Moreover, it has been observed that repeated instrumentation in urethral stricture management procedures can cause fibrosis formation (Waxman & Morey, 2006). Although many antifibrotic drugs, such as halofuginone, mitomycin C, and bitoxin A, have been applied in the treatment of urethral strictures, they have proved to be of little benefit (Tian *et al.*, 2014).

1.4. Regenerative Medicine & Tissue Engineering

To offer alternative approaches in hypospadias treatment aimed at decreasing complication recurrence incidence and reducing morbidity at donor and recipient sites, efforts have been made to realize novel Advanced Therapy Medicinal Products (ATMPs). One of the most promising new medicine fields is the area of cell therapies and their use in regenerative medicine. Regenerative medicine techniques exploit the tissue regenerative capacity guaranteed by the presence of adult tissue stem cells, having a limited differentiation. They are committed to produce a single or few tissue-specific cells types able to repair wound and to maintain physiological turnover. These new technologies hold significant promise for groundbreaking, and potentially therapeutic treatments for some of the most troubling diseases. Tissue engineering techniques can take advantage of stem cell capability to originate a tissue for restoring, correcting and modifying functions. Three main approaches for repair are employed in urethral tissue engineering: reconstruction using cultured autologous cells only, use of biomaterials called scaffolds or matrices, or a combination of both techniques using cell-seeded scaffolds. A scaffold is a biocompatible, biodegradable, bioresorbable device promoting seeded cells proliferation and native cells ingrowth when implanted. Cell-seeded scaffolds can resist mechanical forces, unlike cell-only constructs, that are often too vulnerable to be transported or surgically handled (de Kemp *et al.*, 2015). An ideal biomaterial for urethral reconstruction should ensure secure

attachment for a well-ordered epithelial cell layer to the luminal surface while providing a substrate with a suitable porosity for a fibroblast support feeder layer and keratinocytes growth. It should also provide adequate mechanical support and prevent premature collapse before *in vivo* grafting has completed. Formulations employing human fibrin can have these fundamental qualities, and they have been extensively used in the past decade, demonstrating the possibility to culture epithelial cells in the presence of this natural substance (Macasev *et al.*, 2011; Sese *et al.*, 2011). Fibrin supports have also been employed for ATMP productions, improving manageability and product application (Rama *et al.*, 2001).

1.4.1. Epithelial stem cells in ATMPs development

With the aim of developing a stem-cell based ATMP for the treatment of severe hypospadias patients, cultured tissue supplied with stem cells can be employed for this purpose, since they can engraft and persist at the desired location, self-renew and restore missing functionality. In fact, a characteristic feature of stem cells is their ability to self-renew through proliferation. Consequently, it has been assumed that cells with high *in vitro* growth potential represent stem cells. Indeed, the *in vitro* morphological and growth characteristics of isolated cell populations have been used to evaluate stemness. Cell size could predict human keratinocytes ability to form clones *in vitro* (Barrandon & Green, 1985). As established for other squamous epithelia (Barrandon & Green, 1987), the proliferative compartment of the human oral and urethral epithelia contains three types of clonogenic keratinocytes, referred to as holoclones, meroclones and paraclones *in vitro* (Corradini *et al.*, 2016). Holoclones possess stem cells characteristics including self-renewal ability (De Luca *et al.*, 2006), telomerase activity (Dellambra *et al.*, 2000) and an outstanding proliferative potential (Pellegrini *et al.*, 1999). Paraclones have a very limited proliferative ability and have the properties of transient-amplifying (TA) progenitors. Meroclones have an intermediate proliferative potential. Clonal conversion is the unidirectional transition from a holoclone to a paraclone that occurs during serial cultivation. These clones can be isolated at single-cell level and cultured in suitable culture conditions (Barrandon & Green, 1987). The most reliable tool to evaluate the stem cell content of a specific stratified epithelium is clonal analysis. The method developed to produce numerous human keratinocytes by cultivation from a small biopsy (Green *et al.*, 1979) has led to the first cultured epidermal graft application to

regenerate epidermis of humans suffering from third-degree burns (O'Connor *et al.*, 1981). Later, a new method came along for posterior hypospadias treatment performing urethral reconstruction with autologous graft employing urethral epithelial cells. The technique offered functional improvement over the usual skin grafting, since the application of skin grafts in the urethra results in hair growth, sebaceous secretions, and multiple late fistulas. The epithelium was able to sustain physiological urination and erections (Romagnoli *et al.*, 1990). This technique achieves urethra restoration without employing bladder epithelium, which requires an invasive bladder surgery (Zhong-Chu *et al.*, 1981). However, it is not always possible to retrieve cells to be cultivated from the urethral site, since the urethra could be scarred or totally absent in the most severe cases.

1.4.2. Oral mucosal and urethral epithelia

Epithelial tissues are classified by the number of cell layers and by cell shape and functions. The three principal shapes associated with epithelial cells are squamous, cuboidal and columnar. By layer, epithelia are classified as either simple, unilayered, or stratified epithelium, multi-layered. When simple columnar epithelial cells are viewed in cross section showing several nuclei appearing at different heights, the epithelium is described as pseudostratified columnar epithelium. Transitional epithelium has cells that can change from squamous to cuboidal. Oral mucosa consists of stratified squamous epithelium. In humans there are two forms of oral mucosa: the keratinized oral mucosa, namely the masticatory and the specialized mucosae, and the nonkeratinized oral mucosa comprising the lining mucosal tissues (Jones & Klein, 2013). The nonkeratinized lining mucosal tissue is a stratified squamous epithelium with an underlying connective tissue known as the *lamina propria* (Fig.1.4A). The nonkeratinized epithelium is required to have the appropriate flexibility to accommodate chewing, speech or swallowing. Oral mucosal epithelium has a high regenerative ability to react to daily damages due to chewing, and epithelial stem cells are responsible of oral mucosal regeneration and repair processes. Cell division in oral epithelial cells takes place exclusively in the basal layer. The committed cells undergo a differentiation process after dividing that leads to structural keratin proteins expression and intracellular organelles loss as the cells move superficially, begin to flatten and are eventually lost from the surface (Adams, 1976). The male urethra is divided into four parts.

The urethral epithelium in the prostatic urethra starts as a transitional epithelium, known as the urothelium, as it exits the bladder. This stratified epithelium consists of multiple cell layers which can contract and expand to adapt to the appropriate distension degree. Further along, the membranous and bulbar urethras are composed by pseudostratified columnar epithelium, which distally in the penile urethra becomes stratified squamous epithelium, as it approaches the urinary meatus. The penile urethra is contained in the corpus spongiosum of the penis (Fig.1.4B).

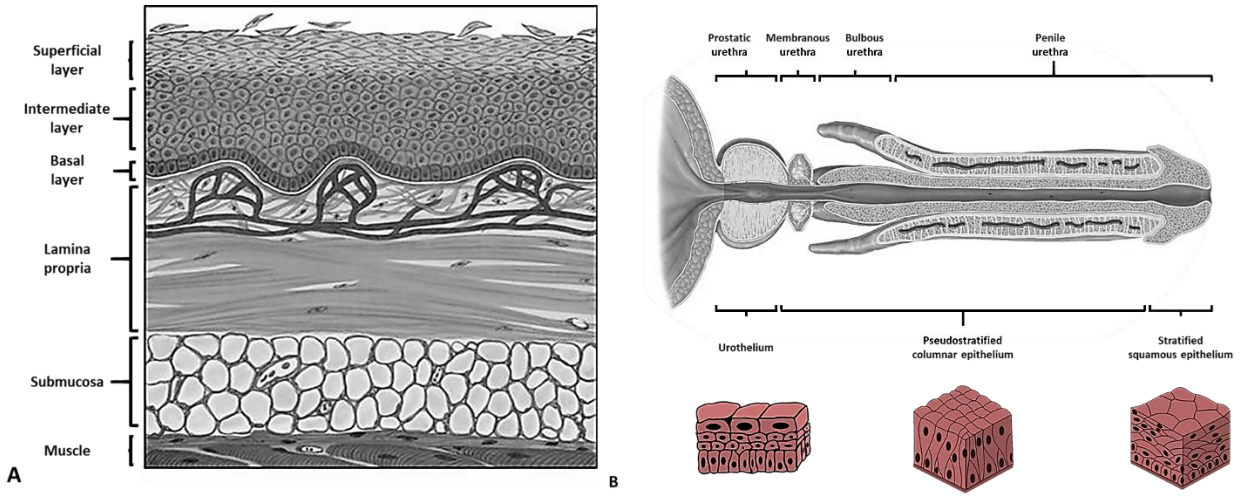

Figure 1.4. ***(A) Nonkeratinized stratified squamous lining mucosa histology.*** *Superficial, intermediate and basal layers overlying the lamina propria. A deeper submucosa overlays muscle tissue. .****(B) Male urethra anatomy and histology.*** *The prostatic urethra is lined with transitional stratified epithelium. The membranous and the bulbous urethras are lined with pseudostratified columnar epithelium. The penile urethra is lined with pseudostratified columnar epithelium proximally and with stratified squamous epithelium distally.*

1.4.2.1. Keratins

The intermediate filament proteins in the keratin group are almost exclusively found in epithelial cells. They are expressed in a tissue-specific and differentiation-dependent manner. These fibrous proteins represent a large family of homologous proteins assembled to form intracytoplasmic cytoskeletal structures. They are usually bundled as tonofilaments (Moll *et al.*, 2008) and are critical for epithelial cell integrity and mechanical stability via cell-cell contacts, as well as protection from apoptosis, stress and injury, and intracellular signal transduction. Keratins are classified as acidic type I or basic/neural type II keratins. Keratins constitute their filamentous conformation by heteropolymeric pair formation of type I and type II molecules with a 1:1 ratio. This association is so essential that single keratin proteins deviating from equimolar type I/II

amounts are rapidly degraded. Within each category, keratins are numbered in order of decreasing size, from low to high molecular weight.

1.5. GMP & Translational medicine

Stem cells and TA cells extracted from an oral mucosa biopsy for an ATMP development must be grown in an *in vitro* culture system strictly under good manufacturing practice (GMP) compliance. The advances in the knowledge of tissue damage and regeneration combined with progresses in the adult stem cell biology field, can provide long-term solutions for the treatment of hypospadias patients. The proposed ATMP serves urethral reconstruction using fibrin, a natural, absorbable, and biodegradable biomaterial, as a cell-seeded scaffold. This scaffold can resist mechanical forces and allows transport and surgical handling and prevents premature collapse before grafting has completed. As a result of a suitable and controlled porosity, it provides the right substrate allowing fibroblast feeder layer deposition and cultivated human oral mucosa keratinocyte stem cells proliferation. It also ensures secure grafting for a well-ordered epithelial cell layer. The transplantation of a novel and innovative ATMP based on a biodegradable scaffold seeded with oral mucosal stem cells can be of great help for failed hypospadias repair treatment patients. As any other drug, ATMP requires detailed manufacturing specifications and should be produced ensuring suitable quality standards. ATMPs including tissue engineering are regulated in the European Union (EU) by established directives such as the 536/2014, 2001/83/EC, and 2009/120/EC directives, allowing European patients to access a safe treatments range based on reproducible scientific grounds. Nonetheless, rules adapted for chemical molecule manufacturing have been applied with difficulties to this new medicine area, and this introduced additional complications in the translation phase. Cell therapy ATMPs are characterized by continuously changing cells, able of proliferation and differentiation. Due to their very different origin from chemical compounds, these products have a very short shelf-life, reducing the time for controls before the ATMP release for clinical use. According to the 1394/2007 European Regulation, selection and transplantation of cells alone are considered minimal manipulations, to the same extent as an organ transplant. In fact, a very different risk applies to cell pathway stimulation, usually obtained through cell-drug contact, and extensive *ex vivo* proliferation typical of ATMPs. Medicinal products must conform to safety standards, meaning both the

product identity assessment and quality certifications. ATMPs should be produced according to GMP and therefore it is required a cell factory with an implemented manufacturing process, from biopsy receipt to final product release. GMP consists of a set of rules describing methods, equipment and means for production management. Therefore, the quality system should be adequately resourced with competent personnel, and suitable facilities. The manufacturing protocols translation to GMP rules guarantees product consistency and batch-to-batch production reproducibility, full reagent traceability, and cross-contamination absence through in-process controls (IPCs) implementation. In addition, GMP compliance is achieved with a series of documentations, such as Standard Operation Procedures (SOPs), an instruction set helping workers to carry out routine operations for efficiency achievement, quality output and performance standardization. Even though each batch is different due to autologous origins, all produced batches must comply to defined quality standards. For this instance, Master Batch Records (MBRs) describe how production is taking place to assure batch-to-batch uniformity. Tools and manufacturing process validation for reproducibility process demonstration are also met. Standardization and examination of a series of parameters, such as manufacturing IPCs, regulatory documents, and patient's selection, is important to conduct an accurate clinical study and to obtain clear results with minimal variables, and these aspects are always factored in planning a clinical trial. Where applicable, donor site, starting tissue and surgical tools characterizations, *in vivo/vitro* cells identification, and regulatory certifications should be all well assessed in urethral reconstruction clinical studies. However, IPC manufacturing process regulations, follow-up analysis standardization, and pharmacovigilance are not always considered when planning a clinical trial. Moreover, it is important to note that biomaterial characterization and biocompatibility, patient selection, and shipping condition controls are as important as any other parameters, and therefore should always be as standardized as possible, even if they were not always addressed in urethral reconstruction clinical studies (Romagnoli *et al.*, 1993; Barbagli *et al.*, 2006; El-Kassaby *et al.*, 2008; Ram-Liebig *et al.*, 2017).

1.5.1. Quality assurance

The 2001/83/CE Directive sets up quality, safety, and efficacy requirements for any medicinal product. The European Medicine Agency (EMA) periodically updates the requirements for each medicinal products class, such as ATMPs. As far as concern quality, any ATMP such as those based on stem cells must have the required identity, purity, potency, and stability levels. Safety and efficacy must be demonstrated at both preclinical and clinical levels during clinical development. All of this is done in order to obtain a well characterized and reproducible product. This goal is achieved with detailed, validated and severe IPCs assuring product quality. The starting donor material is composed by multiple cell populations that can be very different from the final product cells. Identity tests can identify patient cells in the final product cells carrying out the therapeutic effect. Final product characterization and definition is achieved by expression marker profiling. Purity tests are aimed to verify the level of impurities. Any drug product (DP) substance different from the active ingredient may be regarded as an impurity. The manufacturing process of a cell based ATMPs can include different reagents, such as serum, antibiotics, and a feeder layer such as that based on irradiated 3T3 fibroblast cell line derived from Swiss albino mouse embryo (Todaro & Green, 1963) and needed to support oral mucosa keratinocyte growth. As these reagents may cause adverse effects or immune reactions on the patient, they should be reduced to a minimum, while maximizing active components, in order not to dampen therapeutic activity. Their safety should be evaluated in preclinical testing. Potency is the quantitative measure of the biological activity based on the product clinical effect. Therefore, biological characterization is essential in potency assessment. Tests to detect potency predictive markers during preclinical studies help in addressing this matter, but only data from clinical trial will allow to confirm the selected markers consistency.

1.5.2. Preclinical studies

Traditional drugs are characterized by a series of preclinical studies both *in vitro* and *vivo* to evaluate toxicity, pharmacodynamics and pharmacokinetics. The use of a xenograft transplant on an animal model would trigger immune responses, requiring the co-administration of immunosuppressive therapy to prevent graft rejection. This setting is not representative of the clinical situation in which the autologous ATMP would be employed because patients will not

receive immunosuppressive therapy following ATMP administration, since immunosuppressive drugs would alter the environment and cell survival, compromising product efficacy. Since the pig is a common model for several studies about the digestive (Gonzalez *et al.*, 2015) and the cardiovascular systems and is also highly analogous to humans at a genomic level (Groenen *et al.*, 2012), swine was selected as a suitable animal model to test *in vitro* safety and the treatment efficacy in this study. Porcine epithelia cells were cultured in clinical grade culture conditions to transplant the cells onto a pig to mimic human treatment.

1.6. Fibrosis

ATMP therapeutic success achievement can be implemented if recurrent complications likelihood can be predicted. Patients could have the possibility to be evaluated for biomarkers associated with the high stricture treatment failure rate. Inflammatory status is associated with scar formation, one of the hallmarks of fibrosis in stricture progression. As noted, urethral stricture refers not only to a scarring process of the urethral mucosa, but also to the surrounding spongy tissue of the corpus spongiosum (Lumen *et al.,* 2009), since the healing process is not limited to the site of injury but involves the majority of periurethral tissue and corpus spongiosum (Hofer *et al.*, 2014). It could therefore be advisable to know if the urethral stenoses are likely to occur in patients undergoing hypospadias repair treatment and to recur in treated USD patients, in order to identify if treatment responsiveness can be assessed before undergoing surgery. In a patient-oriented perspective, with a simple and non-invasive urine collection, patients' proteome can be analyzed and associated to the clinical follow-up performed by physicians after surgery.

1.6.1. Urine proteomics

Urine is an easily accessible biologic fluid that can be retrieved using noninvasive methods, thus eliminating health risks for the donor. Urine protein composition and fragmentation are relatively stable in comparison with other biofluids such as plasma or serum which are prone to proteolytic degradation during and after sampling (Good *et al.*, 2007). Urine is a rich source to identify biological pathways perturbations and organ malfunctions in the human body and has become one of the most widely used clinical samples for biomarker discovery. It is estimated that approximately 70% of urinary proteins are derived from the kidney and urinary tract (Caubet *et al.*, 2009). The identity and quantity of proteins excreted into urine may reflect pathological

conditions that can be traced to the urogenital tract (Pisitkun *et al.*, 2006). Therefore, proteomics studies could aid at the identification of potential urine biomarkers to distinguish different stenotic patient populations. The urinary proteome has been studied with liquid chromatography (LC)- and mass spectrometry (MS)-based technologies. LC is a high-resolution separation method employing inherent protein characteristics, such as mass, isoelectric point, or hydrophobicity (Neverova & Van Eyk, 2005). This method can separate large amounts of analytes on ultra-high-performance LC (UHPLC) columns with high sensitivity and it can also be automated (Niwa, 2008). Many abundant plasma proteins are present at high concentrations in urine specimens (Chen *et al.*, 2012), making it more difficult to detect potential biomarkers present at low concentrations. Antibody-based affinity-depletion approaches can remove several of the most abundant proteins from various bodily fluids in a single step prior to MS investigation, simplifying the analysis (Fisher *et al.*, 2011; Kushnir *et al.*, 2012; Chen *et al.*, 2013). LC techniques can be coupled with different MS instruments types that affect the identification and quantification accuracy and confidence. The high-resolution instrument Q-exactive (Thermo Fisher Scientific), hybrid of quadrupole and orbitrap, may couple to LC for clinical sample analysis including urine. Proteins separated by LC can be quantified employing label-free techniques (Niwa, 2008). LC-MS can identify low-abundance and hydrophobic proteins not seen by two-dimensional electrophoresis (2-DE) and can be used for urine in-depth analysis (Janech *et al.*, 2007). Protein or peptides quantification in large scale is possible only by gel-free MS-based methods which is considered an advantage for these techniques. As LC-MS is time-consuming and sensitive towards interfering compounds, such as salts, and analytes precipitation on column materials, it is not yet applicable for routine clinical diagnostic tests (Liu *et al.*, 2014).

The project aimed to probe the possibility of a new therapy for hypospadias patient treatment, assessing quality, safety and clinical feasibility of an oral mucosa ATMP in compliance with current directives for a clinical study on urethral reconstruction. The study process included the cultured urethra and oral mucosa comparison to determine whether human oral mucosa epithelial cells (MO) could be employed as a substitute for urethral keratinocytes (UK) in tissue engineering. The ATMP is based on MO stem cells seeded on a biocompatible, absorbable, and easy to transport double fibrin scaffold. Moreover, efforts in proteomics investigations of urinary

biomarker have been made, in order to predict the stricture susceptibility. Urinary proteomes have been examined to distinguish patients likely to develop inflammatory-related complications. In the long run, the analysis of those biomarkers could be predictive of the clinical success and can aid at a well-defined patient selection for therapy improvement.

2. MATERIALS AND METHODS

2.1. Donors

Human oral mucosa and urethra biopsies, and urine samples were obtained in accordance with the tenets of the Declaration of Helsinki, and donors provided informed consent. Oral mucosa biopsy was withdrawn from the inner cheek of patient undergoing surgery for urethral stricture treatment with oral mucosa patch. Urethral biopsies were withdrawn from patients either undergoing stricture treatment surgery from the site not affected by the stricture or undergoing sex reassignment surgery for male-to-female. Healthy and urethral stricture-diagnosed urine donors were devoid of urinary catheter. All the donors were not tobacco smokers and did not have any allergic reactions during the month of urine collection. Patient urine donors were diagnosed with recurrent strictures either derived from failed hypospadias repair treatment or other causes not related to hypospadias. Therefore, for proteomics studies patients were categorized into two groups: recurrent stenotic patients with or without hypospadias.

2.2. Cell cultures

Human oral mucosal and urethral keratinocytes, and porcine urethral keratinocytes were obtained by enzymatic processing of the biopsies and cultivated on a feeder layer (FL) of lethally irradiated 3T3-J2 cells (a gift from Prof. Howard Green). Briefly, biopsy samples were cut in small pieces and dissociated in 0.05% trypsin (Thermo Fisher Scientific, Waltham, Massachusetts, USA) and 0.01% 2,2′,2″,2‴-(Ethane-1,2-diyldinitrilo)tetraacetic acid (EDTA) at 37°C for 120 min. Cells were collected every 30 min, plated at a density of $1.5x10^4/cm^2$ onto GMP-certified lethally irradiated 3T3-J2 FL cells at a density of $2.4x10^4/cm^2$, and were cultured in 5% CO_2 and 95% humidified atmosphere. Cells were plated in keratinocyte growth medium (KNO) composed by DMEM and Ham's F12 (EuroClone, Milan, Italy) media at a 2:1 ratio supplemented with 10% Fetal Bovine Serum (FBS; Thermo Fisher Scientific), 4mM glutamine (EuroClone, Milan, Italy), 50IU/mL penicillin/streptomycin (EuroClone), 5mg/mL insulin (Eli Lilly and Company, Indianapolis, Indiana, USA), 0.18mM adenine, 0.4mg/mL hydrocortisone, 0.1nM cholera toxin, 2nM triiodothyronine. 10ng/mL Epidermal Growth Factor (EGF) was added to KNO medium at the first feeding three days after plating (KC medium). Primary cultures were fed every other day with KC medium.

When keratinocyte culture reached subconfluence the epithelium was dissociated at 37°C for 15 min and either frozen at -196°C in freezing medium composed of 10% glycerol (Johnson & Johnson, New Brunswick, New Jersey, USA) in KNO medium, or serially propagated at a density of $6x10^6$ cells/cm^2 until replicative senescence was reached (Pellegrini *et al.*, 1999).

2.3. 3T3-J2 feeder layer

3T3-J2 murine fibroblast cell line was amplified and maintained in Dulbecco Modified Eagle Medium (DMEM; EuroClone, Milan, Italy) supplemented with 10% irradiated Donor Bovine Serum (DBD; Thermo Fisher Scientific). Before being used as feeder layer (FL), cells were subjected to lethal radiation at ~60Gy and then plated.

2.4. Colony-forming efficiency assay

An aliquot of cells ranging from 100 to 1000 cells from each biopsy, at each serial passage, and from clones were plated onto indicator culture dish previously seeded with 3T3-J2 FL, and cultured. Colonies were fixed 12 days later, stained with Rhodamine B (Sigma-Aldrich, St. Louis, Missouri, USA), and examined under a dissecting microscope. Colonies were scored as progressively growing or aborted, as previously described (Pellegrini *et al.*, 1999; Barrandon & Green, 1987). Colony-forming efficiency (CFE) values were calculated as the ratio of number of grown colonies to the number of plated cells, whereas the percentage of aborted colonies is obtained from the ratio between abortive colonies and the number of all colonies grown in the indicator dish. CFE assay allows to distinguish among clonal types according to the number of aborted colonies. Briefly, when 0-5% of colonies were terminal the clone was classified as a holoclone, when 5-95% of colonies were aborted the clone was classified as a meroclone, and if the colonies were aborted for >95%, the clone was classified as a paraclone.

2.5. Clonal analysis

Holoclones, meroclones and paraclones identification was performed through clonal analysis from subconfluent keratinocytes culture. After limiting dilution, single cells were inoculated into 96-multiwell plates containing 3T3-J2 FL cells. After 7 days of culture, single clones were selected under an inverted microscope. Each clone was dissociated with trypsin digestion to obtain single

cells suspension and then divided into two cell culture plate. Half of the clone was plated into an indicator dish and assayed for CFE to define the clonal type. The other half of the clone was cultured on FL.

2.6. Immunofluorescence assays

Epithelial cells cultured on glass coverslips were fixed for 10 min with methanol (MeOH) at -20°C (when staining for K6, 7, 8 and 18) or 3% paraformaldehyde (PFA) at room temperature (RT; when staining for vimentin and wide-spectrum human cytokeratin), permeabilized with 0.2% Triton-X100 in phosphate buffered saline (PBS) for 20 min at RT, blocked with 2% bovine serum albumin (BSA; Sigma-Aldrich, St. Louis, Missouri, USA) for 1h at RT, and incubated overnight (ON) at 4°C with the following primary antibodies (Abs) diluted in blocking solution: 1:100-diluted anti-K6 (Abcam, Cambridge, UK), 1:00-diluted anti-K7 (Progen Biotechnik GmbH, Heidelberg, Germany), 1:10-diluted anti-K8 (Progen Biotechnik GmbH), 1:200-diluted K18 (Abcam), 1:1000 diluted anti-wide spectrum human cytokeratin (Abcam), or 1:1000-diluted mouse vimentin (BioLegend, San Diego, California, USA). Slides were then incubated with 1:1000-diluted Alexa-Fluor 488 or 568 secondary Abs (Thermo Fisher Scientific) for 30 min at RT. Cultured epithelial cells were trypsinized, centrifuged at a range of 10,000-15,000 cells per slide in a Cytospin™ 4 Cytocentrifuge (Thermo Fisher Scientific, Waltham, Massachusetts, USA) at 450 rpm for 5 min with low acceleration, and fixed for 10 min in 3% PFA at RT. Cytospins were permeabilized with 0.5% Triton-X100 in PBS for 10 min at 4°C, blocked with 2% BSA, double stained with Ventana Discovery XT (Roche Holding AG, Basel, Switzerland) with 1:1000-diluted anti-mouse Vimentin (BioLegend) and 1:1000 diluted anti-wide spectrum human cytokeratin (Abcam) primary Abs. Slides were then incubated with 1:2000-diluted Alexa-Fluor 488 or 568 secondary Abs (Thermo Fisher Scientific) for 1h at RT. Human urethral and mucosal tissues were embedded in an optimal cutting temperature (OCT) compound (Bio Optica, Milan, Italy) on dry ice and frozen at -80°C and cut into 5-7µm sections on a Leica CM1850 UV (Leica Biosystems, Wetzlar, Germany) cryomicrotome. The sections were then thaw-mounted onto glass slides (Superfrost Ultraplus; Thermo Fisher Scientific, Waltham, Massachusetts, USA), fixed for 10 min with MeOH at -20°C, permeabilized with 0.2% Triton-X100 in PBS for 20 min at RT, blocked with 2% BSA for 1h at 37°C, incubated for 30min at 37°C with 1:200-diluted (when staining MO) or 1:2000-diluted (when

staining UK) anti-K6 (Abcam), 1:100-diluted anti-K7 (Progen Biotechnik GmbH), anti-K8&18 (prediluted; Cell Marque Corporation, Rocklin, California, USA) primary Abs. Slides were then incubated with 1:2000-diluted Alexa-Fluor 488 Abs for 30min at RT. For all the staining procedures, nuclei were labeled with 4',6-diamidino-2-phenylindole (DAPI; Roche Holding AG) for 3min at RT and slides were mounted with fluorescent mounting medium (Agilent Technologies). Fluorescence labelled signals were acquired using the Zeiss Axio Imager.A1 fluorescence microscope, or the LSM 510 META laser scanning microscope, where noted (Carl Zeiss AG, Oberkochen, Germany). Image analysis was performed using AxioVision Software v.4.5 (Carl Zeiss AG). For purity assessment the amount of 3T3-J2 contaminant cells is obtained from the difference between total cell number, evaluated by DAPI staining, and wide-spectrum cytokeratin+ cells.

2.7. Transcriptome microarray analysis

Holoclones selected from oral mucosae (N = 2) and urethras (N = 2) clonal analyses were sub-cultivated, feeder-depleted using immunomagnetic beads (Miltenyi Biotec, Bergisch Gladbach, Germany), and collected for total RNA extraction employing a NucleoSpin® miRNA kit (MACHEREY-NAGEL GmbH & Co. KG, Düren, Germany) as per manufacturer instructions. After NanoDrop 1000 Spectrophotometer (Thermo Fisher Scientific, Waltham, Massachusetts, USA) quantification and 2100 Bioanalyzer (Agilent Technologies, Santa Clara, California, USA) quality assessment by capillary electrophoresis rRNA size measurements, 100 ng of total RNA per sample were treated according to the 2-cycle target labeling protocol advised by Affymetrix (Thermo Fisher Scientific). Briefly, of the loaded total RNA, only polyadenylated coding mRNA was reverse transcribed to cDNA; next, *in vitro* 3' transcription (IVT) is performed in order to obtain amplified RNA, while maintaining stoichiometric ratios; during this step, biotin-conjugated nucleotides are used to mark the amplified RNA. Quality assessment is once again performed using the 2100 Bioanalyzer. The Affymetrix Human Genome U133 Plus 2.0 array (Thermo Fisher Scientific) was employed to analyze the entire sample transcriptomes. The arrays hybridization, staining, and scanning were performed using Affymetrix standard protocols as previously described (Salati *et al.*, 2008). The GeneChip Operating Software (GCOS) absolute analysis algorithm (Thermo Fisher Scientific) was used to determine the amount of a transcript mRNA, whereas the GCOS

comparison analysis algorithm (Thermo Fisher Scientific) was used to compare gene expression levels between two samples. Differentially expressed genes (DEGs) were selected from robust multi-array average-normalized data through a supervised analysis, employing the Partek® Genomics Suite® (GS) 6.6 Analysis of variance (ANOVA) model (Partek Incorporated, Chesterfield, Missouri, USA). The selected probe sets displayed a fold-change (FC) contrast ≥2 and a false discovery rate (FDR) ≤0.05 for DEGs in oral mucosa *versus* urethral clones. Upstream regulators were computationally predicted using the Ingenuity® Pathway Analysis (IPA®) software (QIAGEN Silicon Valley, Redwood City, California, USA). Microarray and bioinformatics analysis were performed by Dr. Elisa Bianchi, PhD from Prof. Rossella Manfredini research group.

2.8. Urine sample collection

The first clean-catch mid-stream urine samples from stenotic patients devoid of urinary catheter were collected in the morning without adding stabilizers (see S1.1 for details). Samples were kept at 4°C and processed within 4h of voiding. Urine samples were centrifuged at 5,000 g for 2min to remove cells and debris, and the supernatants were quick-frozen in a dry ice/MeOH bath. To avoid freeze/thaw cycles, one-use 1.5-mL aliquots were stored at -80°C without further manipulation until assay and centrifuged at 9,600 g at 4°C after thawing.

2.9. Urinary protein dosage

Total urine proteins were quantified using Bradford method (Bradford, 1976). Briefly, bovine serum albumin (BSA) was dissolved in phosphate buffered saline (PBS) and standard curves were prepared by dissolving BSA to get 1, 2, 4, 6, 8, and 10 µg/mL final concentrations for Bradford assay. Standard curves had an $r^2 > 0.9906$. Since inter-sample urine concentration variation is broad, multiple dilutions must be employed (Prakash *et al.*, 2008) to precisely measure total urine protein concentration. Samples were quantified both undiluted and diluted by 10-, 20-, 50-fold dilution factors depending on the protein content of each urine sample. Next, 0.5mL of diluted urine sample was added to 0.5mL of Bradford reagent (Bio-Rad Protein Assay Dye Reagent Concentrate; Bio-Rad, California, USA) in each cuvette. The reagent blank consisted of 0.5mL of PBS and 0.5mL of Bradford reagent. The contents were mixed and incubated at room temperature for 5 min and the absorbance read at 595 nm on a DU 730 Life Science UV/Vis

Spectrophotometer (Beckman Coulter Life Sciences; California, USA). The protein content in the sample was calculated using a calibration curve.

2.10. LC-MS/MS analysis

Urine samples were pooled together so to increment the total amount of single proteins. Samples were divided into 3 categories: hypospadic (I) or non-hypospadic (II) patients with recurrent strictures undergoing re-operation procedures, and healthy donors (CTRL) who were never diagnosed with urethral stricture disease. A total of one pool from category I, two pools from category II, and two pools from the CTRL category were analyzed. Each patients pool was composed of 3 patient urine samples, whereas each control group was composed of 5 healthy donor urine samples. From each sample a volume equivalent to 100 µg of total proteins was pooled together with the other samples constituting the respective urine pool. Next, urine pools were concentrated using Amicon Ultra centrifugal filter units (Merck Group, Darmstadt, Germany) with a 5kDa molecular weight cut-off (MWCO) and immunodepleted employing Seppro® IgY14 spin columns (Merck Group) as per manufacturer instructions to remove abundant proteins hindering detection of trace amount proteins during MS (Fisher *et al.*, 2011; Kushnir *et al.*, 2009; Chen *et al.*, 2013). The 14 depleted proteins were albumin, α1-antitrypsin, IgG, IgA, IgM, transferrin, haptoglobin, α2-macroglobulin, fibrinogen, complement C3, orosomucoid, and apolipoproteins A-I, A-II, and B. After immunodepletion, proteins from urine pools were treated to undergo MS analysis. Briefly, 20 µg of total proteins from each of the immunodepleted urine pools were reduced with dithioerythritol (DTE), alkylated with 2-iodoacetamide, a commonly used agent to bind covalently with the thiol group of cysteine so the protein cannot form disulfide bonds (Anson, 1940), and digested with trypsin. The obtained peptides were desalted and analyzed in nano-liquid chromatography tandem mass spectrometry (nLC-MS/MS) by online ultrahigh performance LC (UHPLC), employing the Q Exactive™ Hybrid Quadrupole-Orbitrap™ Mass Spectrometer (Thermo Fisher Scientific). A 15-cm long, 75µm in diameter, and 1.9-µm ReproSil-Pur 120 C18-AQ resin packed chromatographic column (Dr. Maisch HPLC GmbH, Ammerbuch, Germany) was employed in combination to a gradient of LC-MS water containing 0.1% v/v formic acid (eluent A) and acetonitrile containing 0.1% v/v formic acid (eluent B) for peptide separation, with a 300nL/min flux, from 2 to 40% B in 88min. A 70,000-

resolution in a 300 to 2000Da m/z mass range was employed for full MS acquisition, while the 10 most intense ions (with 2 or 3 charges) were selected for MS/MS fragmentation, employing a 17,500 resolution. Each sample was analyzed in technical triplicate. MaxQuant v 1.6.1.0 software was employed for protein identification and precursor intensity-based and label-free quantification. The Complete Human Proteome 20190605 was employed as reference database. The levels of proteins identified in hypospadic and non-hypospadic patients were compared with their levels in control group and between each other. Statistical analysis on obtained data was performed using the Multiple Experiment Viewer (MeV) v.4.9.0 software to identify significantly differently expressed proteins (DEPs) in the different urine pools having p-values < 0.005 by unpaired t-test. MS and bioinformatics analyses were performed by Annapaola Andolfo, PhD, Proteomics facility manager for the IRCCS San Raffaele Hospital, Milan, Italy. DEPs were selected by a FC ≥ 2 or ≤ -2.

2.10.1. Functional enrichment analysis

DEPs for the hypospadic and non-hypospadic group were analyzed by Gene Ontology (GO) based on the biological process, cellular component and molecular function categories using the Database for Annotation, Visualization and Integrated Discovery (DAVID; Huang da *et al.*, 2009). For determination of protein-protein interactions the Search Tool for the Retrieval of Interacting Genes/Proteins (STRING) database was used. The included interactions sources were both known interactions, such as from databases and experimentally determined, and predicted interactions, such as gene neighborhood, fusions, co-occurrence, peer-reviewed papers text mining, and homology interactions from model organisms.

3. RESULTS

3.1. Epithelia characterization

Oral mucosal and urethral cells have been extracted from biopsies and cultivated. The characterization of the starting material is mandatory from a regulatory perspective to assess tissue replacement feasibility and therefore, investigations were focused on oral mucosa and urethra clonogenic ability, identity marker expression, and stem cell abundance, as well as safety and quality assessments of the final drug product (DP).

3.1.1. Oral mucosa and urethral epithelia clonogenic ability and growth potential

Biopsies were surgically removed from oral mucosa (MO) or penile urethra (UK) of patients, placed in primary containers with transport medium, and transferred to the laboratory within 24h. The culture conditions were modified according to regulatory requests for ATMPs and included clinical-grade hormones and growth factors. Reagents were extensively screened for the contaminants and cytotoxic effects absence. All the sera were irradiated. Epithelial cells were isolated from a total of 43 oral mucosa and 21 urethra biopsies from living donors and cultured *in vitro*. Clonogenic ability, growth potential, marker expression to identify subpopulations in culture, and stem, progenitor, and transient-amplifying (TA) cells abundance were assessed to evaluate the *in vitro* tissue regenerative capacity maintenance. The clonogenic ability is the capacity of a basal cell to produce a colony. Processed UK (N = 10) and MO (N = 43) biopsies had comparable clonogenic abilities of 7.20±3.24% and 2.27±1.94%, respectively. After primary culturing, the colony-forming efficiencies (CFEs) of the two epithelia were still similar, showing a clonogenicity of 54.16±14.02%, and 47.88±23.69%, respectively (Fig.3.1A). The growth potential, namely the capacity to produce cell generations, was maintained for several passages, and then progressively decreased until replicative senescence was reached. The proliferation end occurred after a cell doubling average of 89.83±26.29 for MO (N = 4), 167.13±49.43 for healthy UK (N = 4; Sceberras *et al.*, 2019), and 71.41±21.24 for stricture-affected UK (N = 6) before senescence, proving the absence of immortalization events (Fig.3.1B).

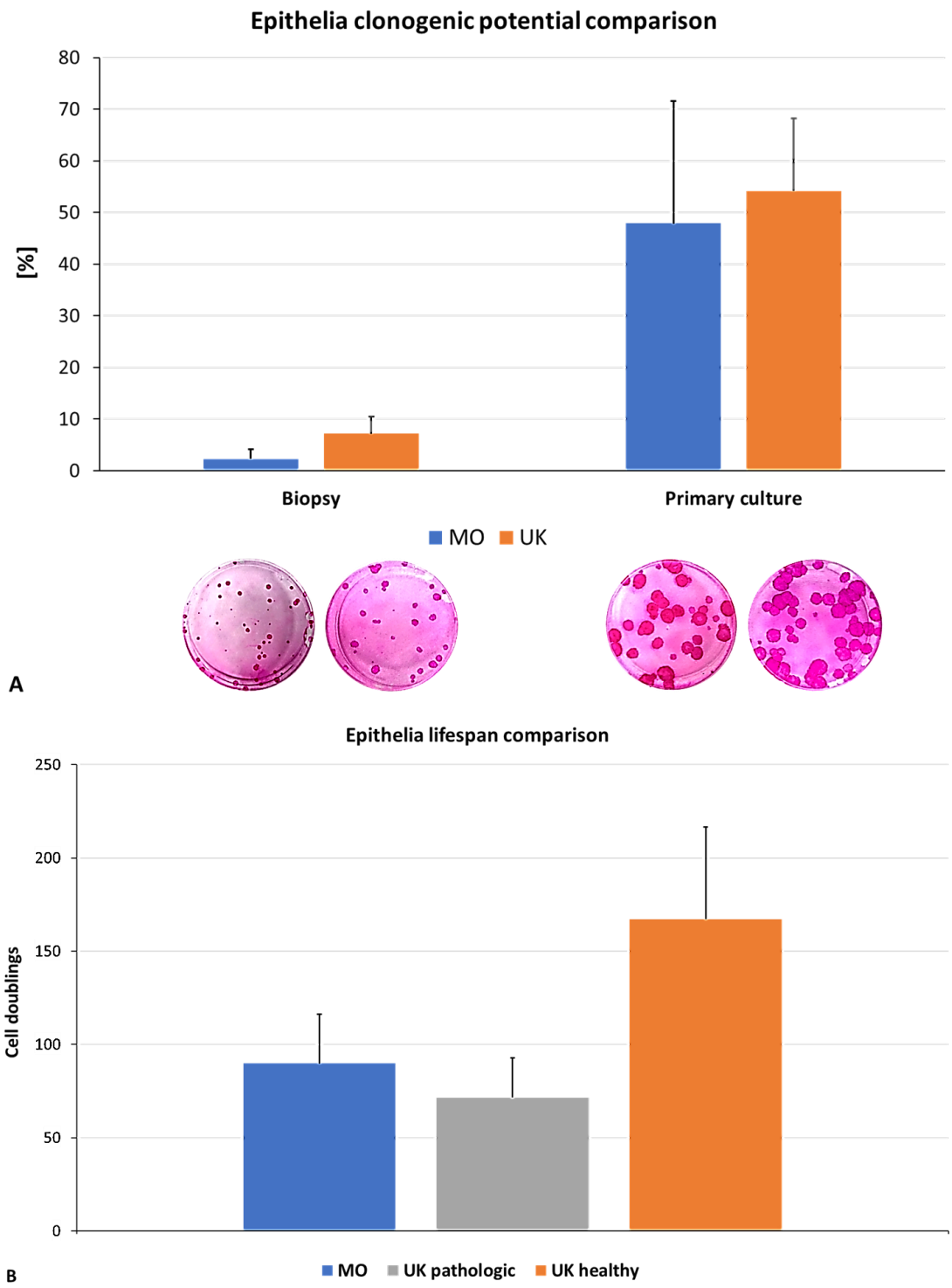

Figure 3.5. ***Epithelial culture characterization. (A) Urethra and oral mucosa clonogenic potentials.*** *Cells extracted from urethral and oral mucosa biopsies were assessed for CFE; keratinocytes primary culturing showed a more elevated CFE than biopsy; the two epithelia had comparable clonogenicities. Difference between MO biopsy and primary culture CFEs is significant for a p-value < 6E-21; difference between UK biopsy and primary culture CFEs is significant for a p-value < 6E-09.* ***(B) Oral mucosa and urethral keratinocyte culture lifespans.*** *Oral mucosa and urethral cell cultures reached replicative senescence proving immortalization events absence during culturing; lifespan length was similar for both epithelia. Difference between UK pathologic and healthy cell doublings is significant for a p-value < 0.01.*

3.1.2. Keratin markers expression

Keratin (K) expression is a feature of epithelial cells. Keratins are part of the cytoskeleton and critical for cellular and tissutal integrity, mechanical stability, and for cell function regulation. The previously characterized differentiation K4/13 pair is *in vitro* and *in vivo* expressed by both urethral and oral mucosa epithelial, as well as the basal K5/14 pair. The basal marker K19 was also detected in both epithelia (Corradini *et al.*, 2016). K6, K7, K8, and K18 were therefore characterized to further investigate their tissue-specific modulation both *in vivo* and *vitro* under mitogenic stimuli in the defined culture conditions. The two epithelia revealed very similar keratin expression patterns. The K6, constitutively expressed in highly proliferative mucosa, was shown *in vivo* and *in vitro* in both tissues, whereas K7 exhibited a different expression *in vivo* and *in vitro*, as only cultured cells showed K7 expression; since the cells are exposed to mitogenic stimuli and behave as in wound healing, several functions are therefore activated (Sun, 2006). The K8, typically expressed in oral malignancies, was negative in cultured oral mucosa, but positive in cultured urethral epithelium. Type I K18 was activated *in vitro* in both urethra and oral mucosa. K18 paired with the type II K8, was not detected in *in vivo* oral mucosa samples, but was activated in urethral *in vivo* samples (Fig.3.2; Sceberras *et al.*, 2019). Altogether, the cytokeratin expression maintained a physiologic tissue- and differentiation-specific location, and regulation pattern, comparable in both urethra and oral mucosa.

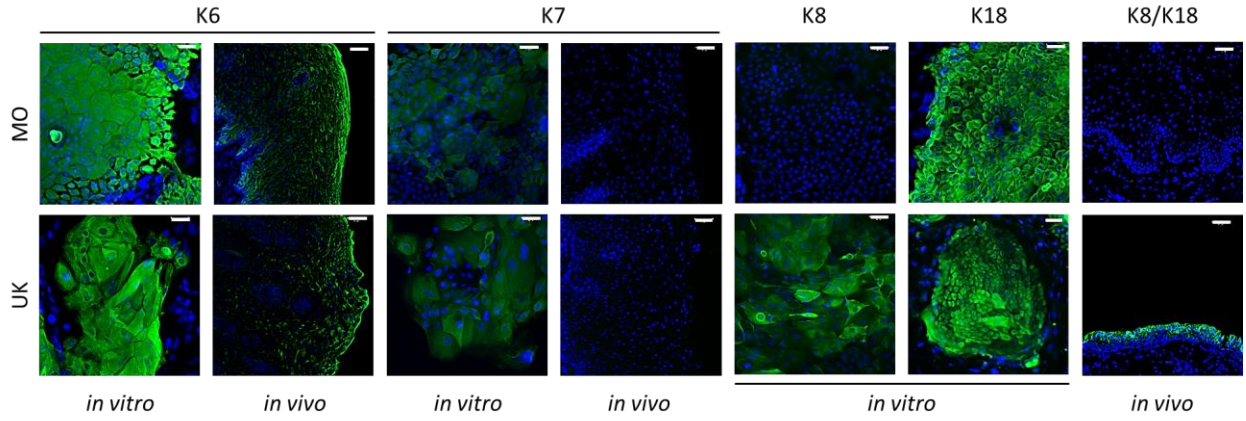

Figure 3.2. ***Keratins expression profiles.*** *Laser scanning microscopy for keratin evaluation in urethral and mucosal samples both* in vitro *and* vivo*. Similar expression pattern was observed for both epithelia. Scale bar 50µm.*

3.1.3. Oral mucosa and urethral epithelia clonal profiling

The lining epithelia proliferative compartment is in the basal layer and contains three identified keratinocyte types with different multiplication abilities: holoclones, meroclones, and paraclones (Barrandon & Green, 1987). The holoclone has the greatest growth potential and is the epithelial stem cell of several epithelia and hair follicles (De Luca *et al.*, 2006). To assess holoclone stem cells, meroclone progenitors, and paraclone TA cells amounts in urethra (N = 5) and oral mucosa (N = 3) epithelial cultures, single cells were isolated from subconfluent cultures. After 7 days of cultivation half of each clone was cultured, fixed 12 days later, and stained to classify clonal type based on aborted colonies relative number. Even though holoclones appeared in a lower amount in urethra, 10.50±6.28%, than in oral mucosa, 19.29±4.27%, these differences could not be considered statistically significant. Paraclone percentages were 23.33±10.65% and 18.28±5.94%, respectively. Meroclone amounts were 66.17±9.49% and 62.42±2.28% of the total analyzed clones, respectively, and they appeared to be the predominant clonal type among the others (Fig.3.3). In agreement with the mass culture cell doubling numbers, holoclones isolated from both epithelia were able to actively proliferate with no evidence of replicative senescence soon after clonal analysis. Meroclones displayed high heterogeneity in their growth potential, and paraclones underwent a very limited cell division number as expected. The three clonal types were similarly represented in both epithelia.

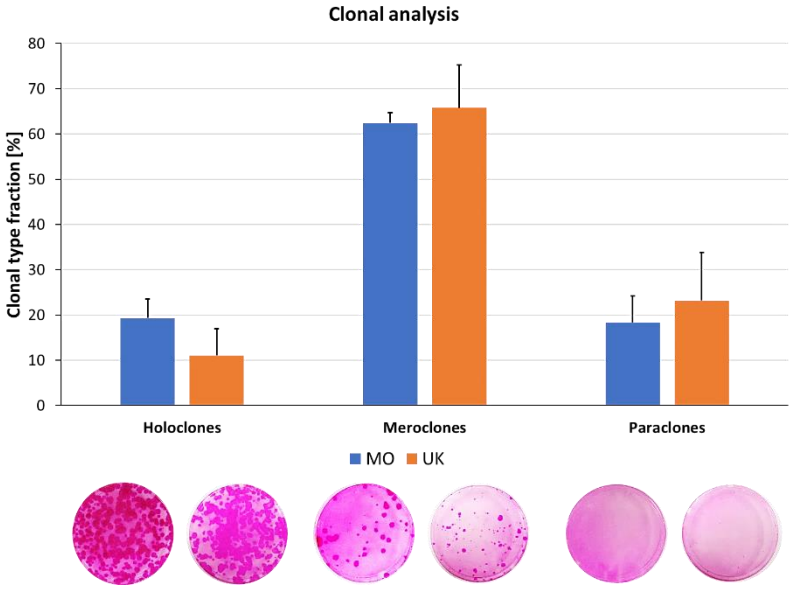

Figure 3.3. ***Clonal analyses to assess cell type amounts.*** *Keratinocytes from urethral and oral mucosal cultures were analyzed in single cells. Stem cells (holoclones), progenitors (meroclones), and TA cells (paraclones) percentage amounts differences between the two cultured epithelia were not significant. Differences between MO holoclones and meroclones, MO meroclones and paraclones, UK meroclones and paraclones are significant for a p-value < 0.001; difference between UK holoclones and meroclones is significant for a p-value < 5E-06*

3.1.4. Stem cell transcriptome

Differences between the two epithelia were further evaluated by microarray transcriptome analysis of the respective holoclone stem cell populations. The gene expression profiles of 15 holoclones isolated from two MO strains, and 4 holoclones from two UK strains were analyzed. 100 differentially expressed genes (DEGs) having a fold-change (FC) ≥ 2 and a false discovery rate (FDR) ≤ 0.05 were identified in oral mucosa compared to urethral holoclones (Fig.3.4A). Of note, Hox genes were downregulated in oral mucosa compared to urethra holoclones. The repression of Hox genes has been shown to preserve the undifferentiated state of stem cells (Biehs *et al.*, 2013). These findings are consistent with stem cell maintenance in culture. *PTGS2* expression appeared to be downregulated in oral mucosa compared to urethra. Notably, its inhibition can prevent urethral strictures development by interfering with the inflammatory processes preceding scar formation (Sciarra *et al.*, 2005). Based on the DEG list and according to current literature knowledge, IPA® upstream regulator analysis proposed transcriptional regulators that could underlie the differential gene expression of oral mucosa and urethra holoclones. Hox genes downregulation in oral mucosa *vs.* urethra holoclones was confirmed by the predicted concurrent inhibitions of the upstream Hox-genes expression epigenetic regulator *KAT6A* (Sheikh *et al.*, 2015), the expression-maintaining epigenetic transcriptional activator *KMT2A*, and the transcription-promoting Hox-cofactor *MEIS1* (Isono *et al.*, 2005; Li *et al.*, 2016). *BMI1* resulted activated and its related inhibition of *HOXA* genes was confirmed by experiments highlighting lower HOXA transcripts levels in oral mucosa compared to urethra. In addition, IPA® upstream analysis highlighted the increased activity of *TP63* in oral mucosa compared to urethra holoclones based on target *AGR2*, *CDKN1C*, and *MPZL2* downregulations, and *IL1B* and *CYGB* upregulations (Fig.3.4B; Sceberras *et al.*, 2019). However, no significant differences were detected in single cells of the two tissues for p63 and BMI-1 protein levels (Corradini *et al.*, 2016), and the differential gene expression in clones could reflect a stem-cell maintenance-capacity difference of oral mucosa *vs.* urethra after cell expansion.

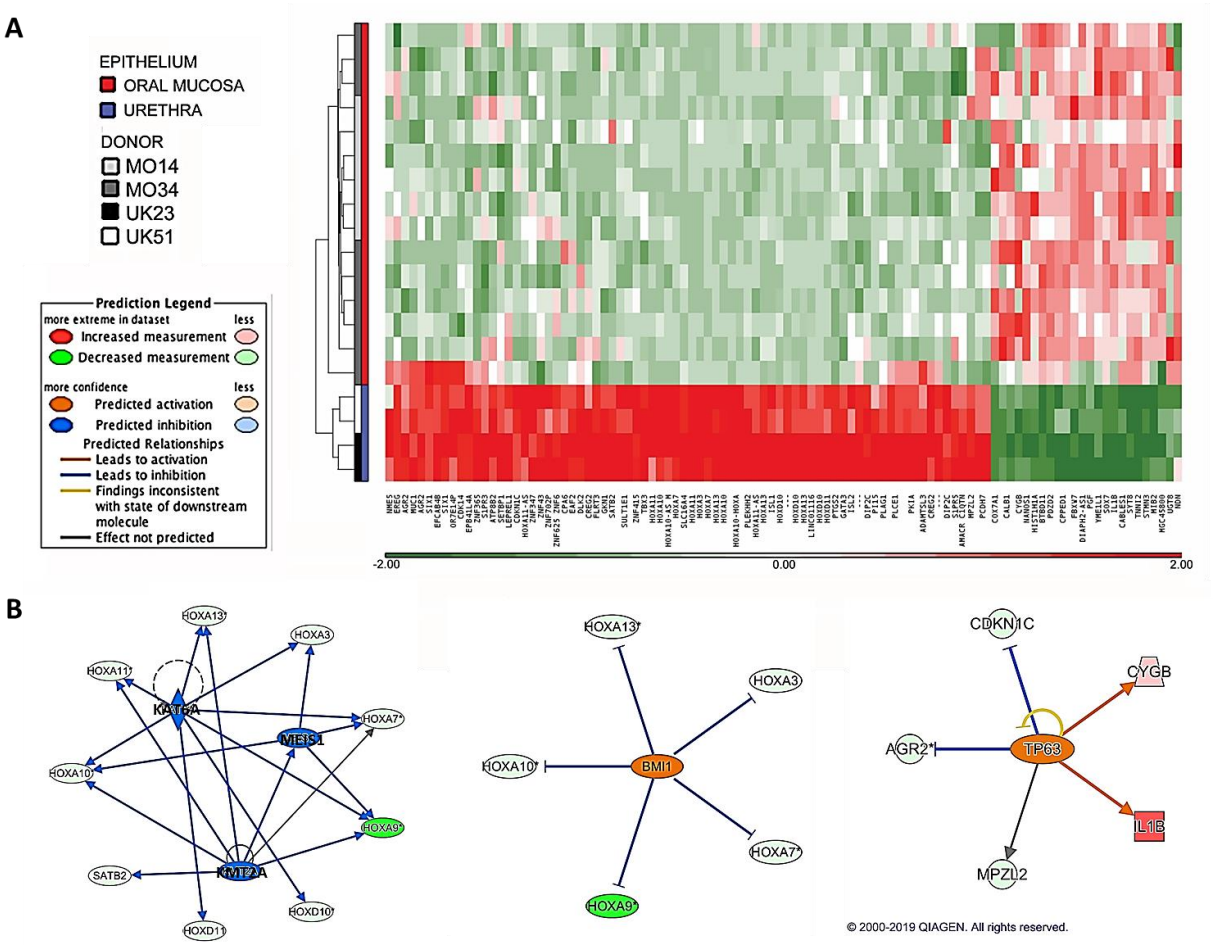

Figure 4. ***Transcriptome microarray analysis. (A) DEG heatmap.*** *DEGs found in oral mucosa* vs. *urethral stem cell transcriptome; red blocks indicate upregulated genes, while green blocks indicate downregulated genes.* ***(B) Upstream regulator analysis.*** *Evaluation to predict the transcriptional regulators that could underlay the differences between the stem cell expression pattern of the two epithelia.* BMI1 *and* TP63 *were predicted to be activated, while* KAT6A*,* KMT2A*, and* MEIS1 *were predicted to be inhibited in oral mucosa* vs. *urethral holoclones. The predicted upregulators had a p-value of overlap < 2.6E-03.*

3.2. Drug product evaluation

After assessing absence of significant differences in regenerative capacity maintenance, markers expression, and stem cells abundance between the two epithelia, oral mucosa was selected for repair and we defined a standardized protocol to cultivate oral mucosal cells on a biocompatible support. The final tissue constructs were obtained on modified fibrin glue scaffolds (EP Patent 1451302) covered by a feeder layer of lethally irradiated 3T3 murine fibroblasts where *ex vivo* autologous human oral mucosal cells expanded to form an epithelium. The constructs were further covered with a different formulation of rapidly resorbable fibrin glue, to reduce friction forces over the epithelium during and after surgery. This double-fibrin scaffold provides

protection during transport and surgical manipulations, enabling continuous adhesion, and preserving the epithelia proliferative potential. Since ATMPs are subjected to extensive assessments by regulatory authorities, quality, safety, and efficacy have been evaluated.

3.2.1. ATMP quality assessment

Safety evaluation and quality control assays were developed to assess the ATMP risk profile. From an oral mucosa biopsy, the drug substance (DS), namely the oral keratinocytes, are extracted to be cultivated. The DP is composed by a cultured oral mucosa epithelium in-between two fibrin scaffolds. Cell type identity, purity, and potency confirmations are regulatory requirements for investigational medicinal product to be used in clinical trials. Cell identity was checked during cell production and banking, and no segregation, major cross-contamination, or 3T3 cell fusion were found after or during culture manipulation. The wide-spectrum human cytokeratin marker was constitutively expressed by oral mucosal cells; therefore, cellular identity maintenance was routinely evaluated through these markers (keratins) *in vitro* and on DS. On the other hand, the purity was evaluated through a murine vimentin marker, not produced by human epithelium. Keratins were constitutively expressed by oral mucosal cells, while murine vimentin was not produced by human epithelium, and it was present in residual feeder cells only (Fig.3.5). Since tissue maintenance and regeneration over time rely on stem cell presence in self-renewing tissues, oral mucosal stem cells regeneration- and proliferation-related markers were considered as good potency candidates, measuring a relevant biological tissue function. Hence, potency was evaluated by nuclear p63 and BMI-1 expression both *in vivo* and in cells processed from DP for comparison (Sceberras *et al.*, 2019). Oral mucosa stem cell clones have higher BMI-1 and p63 levels than transient amplifying clones, and markers expression progressively decreases with replicative senescence and differentiation (Corradini *et al.*, 2016).

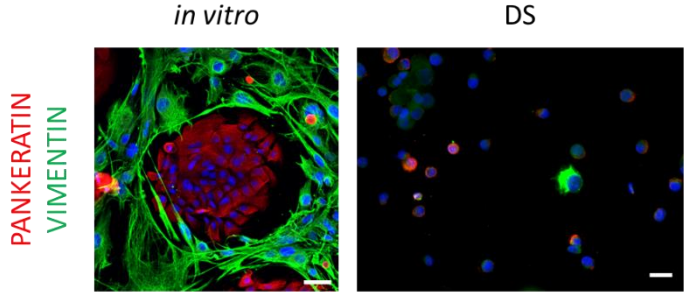

Figure 3.5. ***Purity assessment.*** *Vimentin-expressing FL cells (green) surround pankeratin (wide-spectrum human cytokeratin)-expressing epithelial colonies (red) in* in vitro *cultures (laser scanning microscopy); residual vimentin expression is found in low amounts in DS and in FL cells only. Cells nuclei were stained with DAPI (blue). Scale bar 50µm.*

3.2.2. Preclinical porcine *in vitro* studies

Autologous cell based ATMPs cannot be evaluated as traditional drugs and therefore *in vivo* preclinical studies evaluating toxicity, pharmacodynamics, and pharmacokinetics were not possible. The pig is considered a common model for several studies due to the high analogy to humans at a genomic level (Groenen *et al.*, 2012). Therefore, swine was selected as a suitable animal model to test the safety and the efficacy of the treatment. It would require an immunosuppressive therapy administration to prevent graft rejection, since the xenograft transplant use on the animal model would trigger an immune response. However, the immunosuppressive drugs would alter the environment and the cell survival, making this practice not representative of the clinical situation and compromising the product efficacy. On this basis, urethral porcine epithelia were cultured in GMP conditions to transplant the porcine cells onto a pig to mimic the natural engraftment for urethral reconstruction. Therefore, porcine urethral biopsies (pUK; N = 3) were processed and compared with human urethral biopsies (hUK; N = 10). Cell yields were similar and not significantly different, showing biopsy yields of ~920,000 cells/cm^2 for both human and porcine urethras, and primary culture yields of ~110,000 and ~130,000 cells/cm^2, respectively (Fig.3.6A). pUK and hUK biopsy clonogenicities were similar, 6.23±5.25% and 7.20±3.14%, respectively. However, a wide discrepancy was observed in the subsequent cell expansion, and porcine cells revealed low responsiveness to culture conditions and mitogenic stimuli, maintaining a very low clonogenic capacity: 4.13±1.64% compared to the human cell clonogenicity of 54.16±14.02% (Fig.3.6B; Sceberras *et al.*, 2019). Porcine urethral keratinocytes did not react to the clinical-grade culture conditions and made the porcine *in vitro* model useless for the safety studies, and therefore its application was discontinued. Hence, safety tests were performed on cultured human cells including soft agar colony-formation assay to confirm the *in vitro* anchorage-dependent cell growth, growth factor-dependence assay to predict uncontrolled cell growth, and karyotype analysis confirming the absence of chromosomal abnormalities under the selected culture conditions (Sceberras *et al.*, 2019).

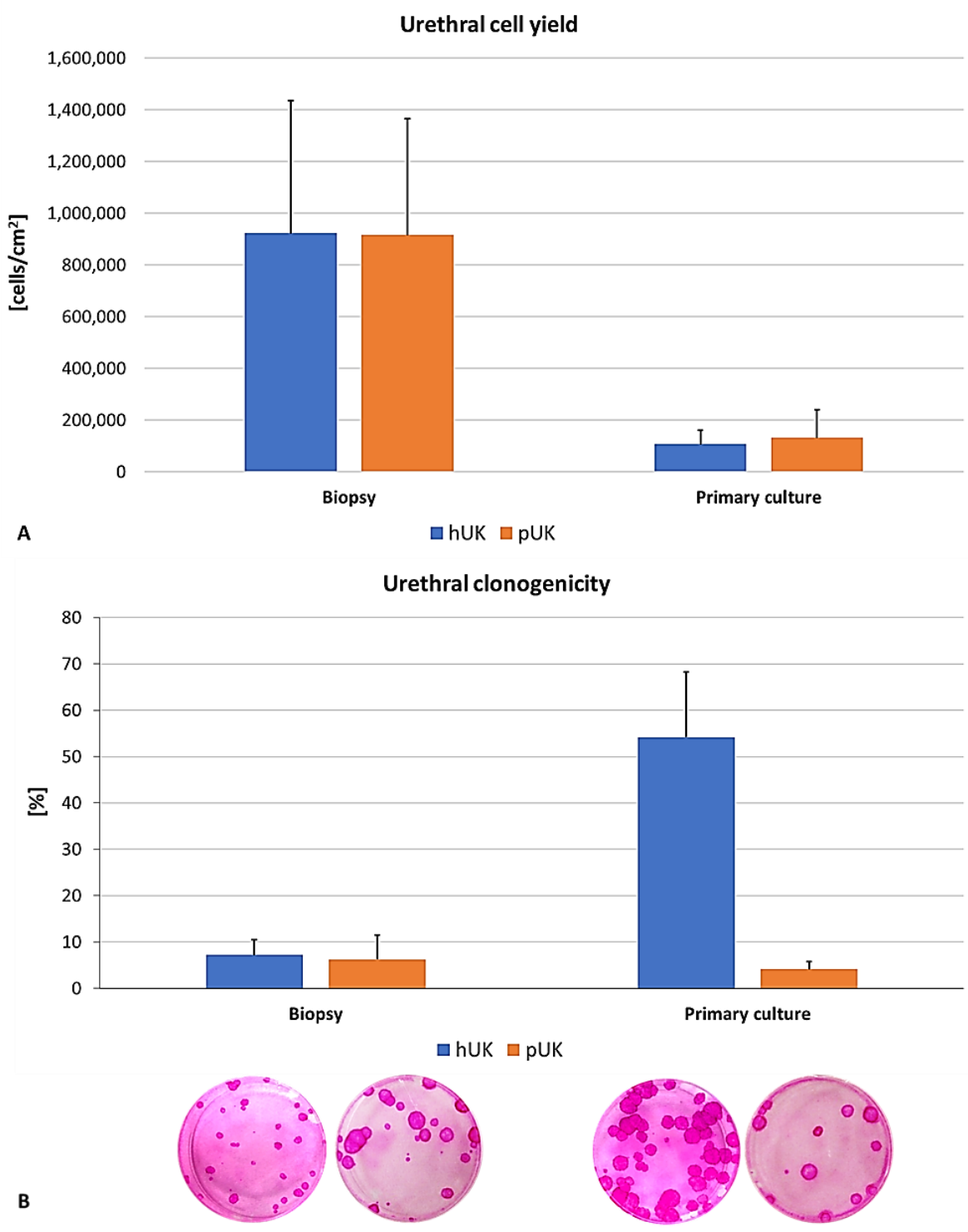

Figure 3.6. ***Preclinical* in vitro *assessments. (A) Urethral cell yields from human and porcine urethras.*** *Cells extracted from human and porcine urethral biopsies and primary cultured cells were similar in yields. Differences between human biopsy and primary culture cell yields were significant for p-value < 7E-05; differences between porcine biopsy and primary culture cell yields were significant for p-value < 0.05.* ***(B) Human and porcine urethral cells clonogenicity comparison.*** *CFE of cells extracted from biopsies resulted similar between the two species. However, pUK primary cultures were not responsive to the clinical-grade environment and therefore keratinocytes could not be serially grown. Difference between human and porcine primary urethral culture clonogenicity was significant for p-value < 1E-06*

3.3. Urinary proteome profiling

Fibrosis-derived urethral stenosis is one of the main complications after primary hypospadias treatment. Therefore, in order to implement ATMP therapeutic success, the inflammatory profile of patients was investigated to find markers related to stricture susceptibility. Urinary proteomes have been examined to distinguish patients developing inflammatory-related complications from healthy controls. The biomarkers analysis can be predictive of the clinical success and can aid at a well-defined patient selection for therapy optimization. Urine was investigated by means of nano-ultrahigh performance liquid chromatography tandem mass spectrometry (nUHPLC-MS/MS) to describe proteome profiles of healthy controls and patients undergoing urethral stricture surgery. Urethral stricture patients were all reminiscent of an inflamed environment since they underwent multiple surgeries after previously failed treatments. Urine samples from recurrent urethral stricture patients were grouped depending on whether they were hypospadic (I) or non-hypospadic (II), and each group resulted from pooling different samples to increase the total amount of proteins as follows: 3 samples from category I were pooled together, and a total of 6 samples from category II were grouped in 2 different pools composed by three patients each. The control group (CTRL) was divided into 2 pools, each composed by five healthy donor samples. From each sample a volume containing 100 µg of total proteins was obtained and then immunodepleted to remove the most abundant proteins hindering trace proteins detection (Tab.3.1). For each pool, a total of 20 µg of immunodepleted proteins were loaded for label-free LC-MS/MS analysis. A total of 874 proteins were identified and quantified comparing pools I *vs.* CTRL, 864 proteins comparing pools II *vs.* CTRL, and 707 proteins comparing pools I *vs.* II. Statistical analysis on data showed 132 (Fig.S2.1), 126 (Fig.S2.2), and 69 (Fig.S2.3) significantly different expressed proteins (DEPs) with p-value < 0.005. In hypospadias patients 100 DEPs had a FC ≥ 2 or ≤ -2 compared to control (Tab.S3.1), whereas in non-hypospadias stricture patients, the DEPs were 69 (Tab.S3.2). After evaluation of overlaps, 22 proteins appeared to be significantly different between stenotic hypospadic patients compared to non-hypospadic patients, but they did not show significant expression differences compared to the control population (Fig.3.7). Therefore, these proteins have not been associated with the disease and

excluded from further analysis, and significantly DEPs in hypospadic *vs.* non-hypospadic recurrent stricture patients with a FC ≥ 2 or ≤ -2 decreased from 45 to 23 (Tab.S3.3).

Pool type	Sample	Immunodepletion yield (µg/mL)
I	Hypospadic	1.14
II	Non-hypospadic (a)	3.07
	Non-hypospadic (b)	0.36
CTRL	Healthy donors (a)	0.67
	Healthy donors (b)	2.18

Table 3.1. ***Protein yields after immunodepletion.*** *A volume equivalent to 100µg for each sample was grouped together to form a pool to be MS-analyzed. Before analysis, each pool was immunodepleted to remove abundant proteins hindering MS detection of trace proteins.*

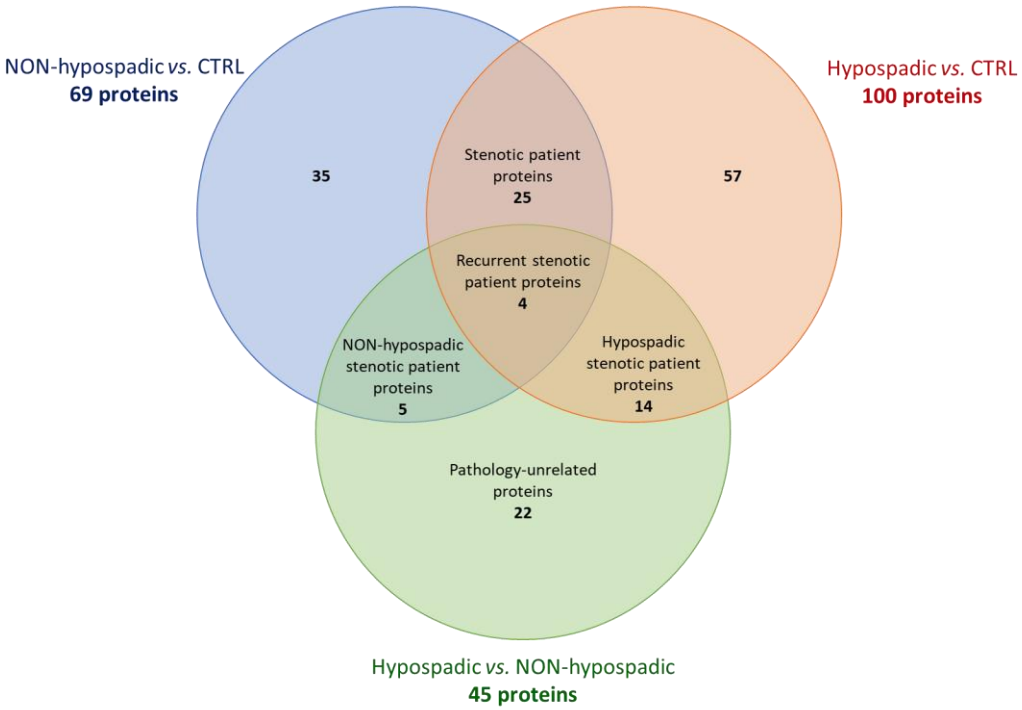

Figure 3.7. ***Identified differential proteins overlap evaluation.*** *DEPs in urethral stricture hypospadic patients compared to controls (red), non-hypospadic patients compared to control (blue), and hypospadias* vs. *non-hypospadias patients (green). Overlap between blue and red sets comprises proteins modulated in all the investigated stenotic patient population; overlap among the three sets comprises proteins modulated in all type of patients undergoing recurrent surgery due to previously failed treatments.*

3.3.1. Functional enrichment analysis

Differential proteins functional enrichment analysis was performed using DAVID (Huang da *et al.*, 2009). Differential proteins were classified into biological processes (BPs), cellular components (CCs) and molecular functions (MFs). A significance threshold of p-value < 0.05 was set in all the lists. 16 and 53 BPs were found to be significantly represented in non-hypospadic and hypospadic urethral stricture patients, respectively. The number of statistically significant CCs was 12 and 14, respectively, and there were 9 and 20 statistically significant MFs, respectively (Tab.S3.4). In the BP category, endopeptidase activity negative regulation, immune response regulation, and basement membrane (BM) organization were represented in both stenotic hypospadic and non-hypospadic patients compared to control. Extracellular matrix (ECM) disassembly, innate immune response, and cellular protein metabolic process were the most statistically significant BPs in non-hypospadic urethral stricture patients (Fig.3.8). Independently enriched BPs were receptor binding negative regulation, 76.15 fold-enrichment, and BM organization (66.63) for the non-hypospadic patient type, whereas renal output regulation by angiotensin, coagulation (176.76 each) and natural killer cell differentiation involved in immune response negative regulation (117.83) were enriched in the hypospadic recurrent-stenotic patients. Interestingly, in these patients, BPs such as response to reactive oxygen species, inflammatory response, and cytokine secretion were represented, possibly indicating altered inflammatory status presence (Fig.3.8B).

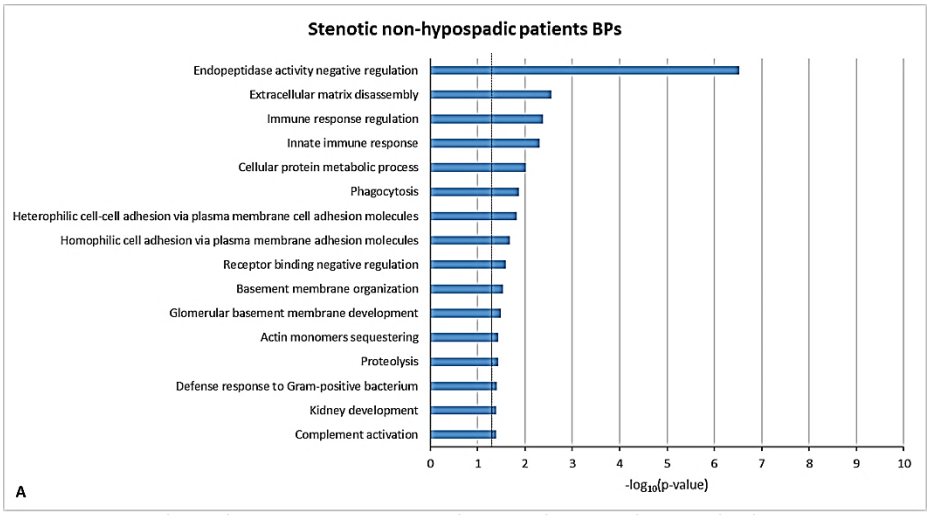

Figure 3.8A. ***Biological processes represented in non-hypospadias urethral stricture patient proteome.*** *Dashed black line indicates the p-value threshold of 0.05.*

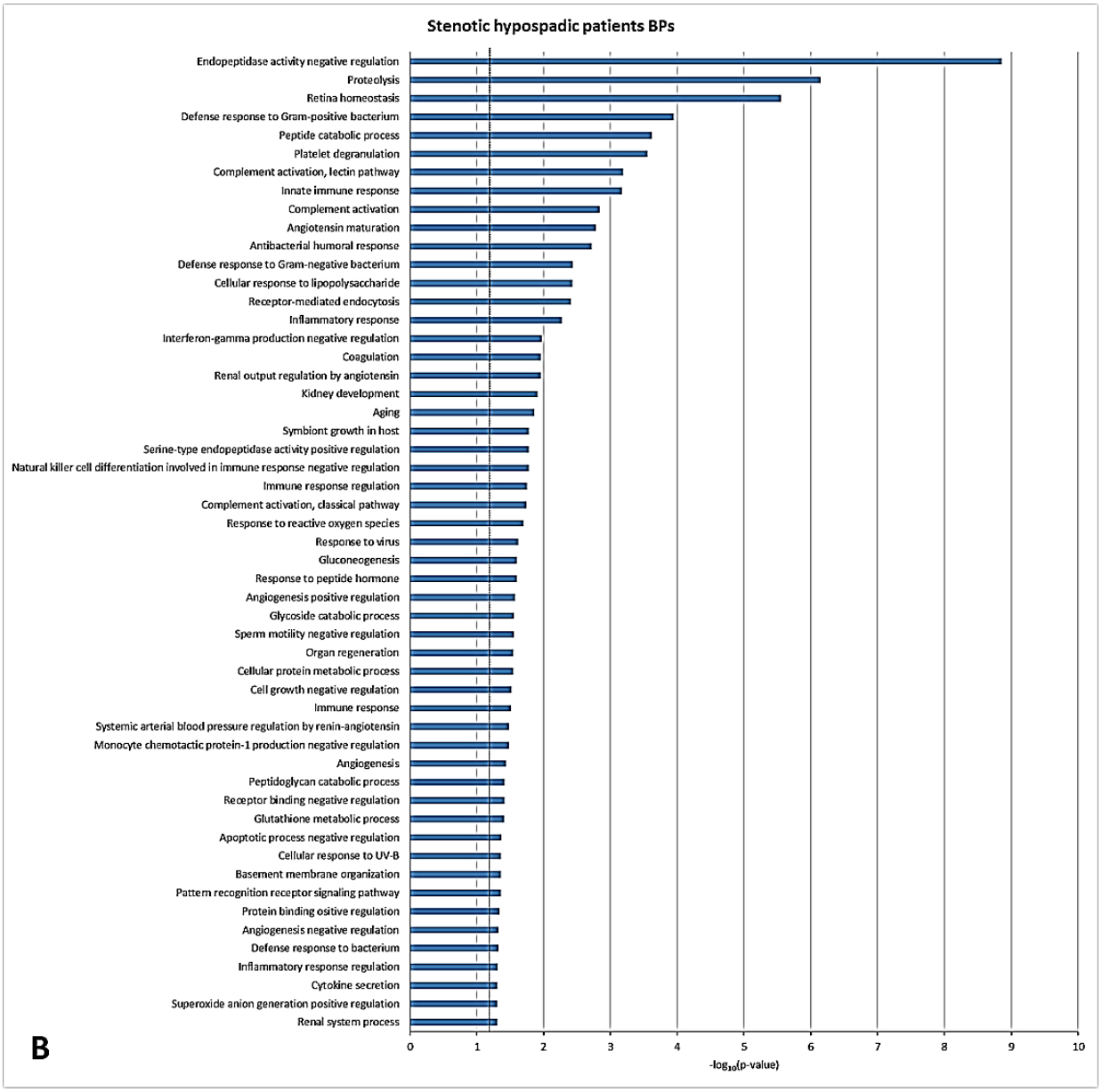

Figure 3.8B. ***Biological processes represented in non-hypospadic stenotic patients.*** *Dashed black line indicates the p-value threshold of 0.05.*

Extracellular exosome, space, and region, blood microparticle, and ECM were represented CC in both hypospadias and non-hypospadias stenotic patients compared to control (Fig.3.9).

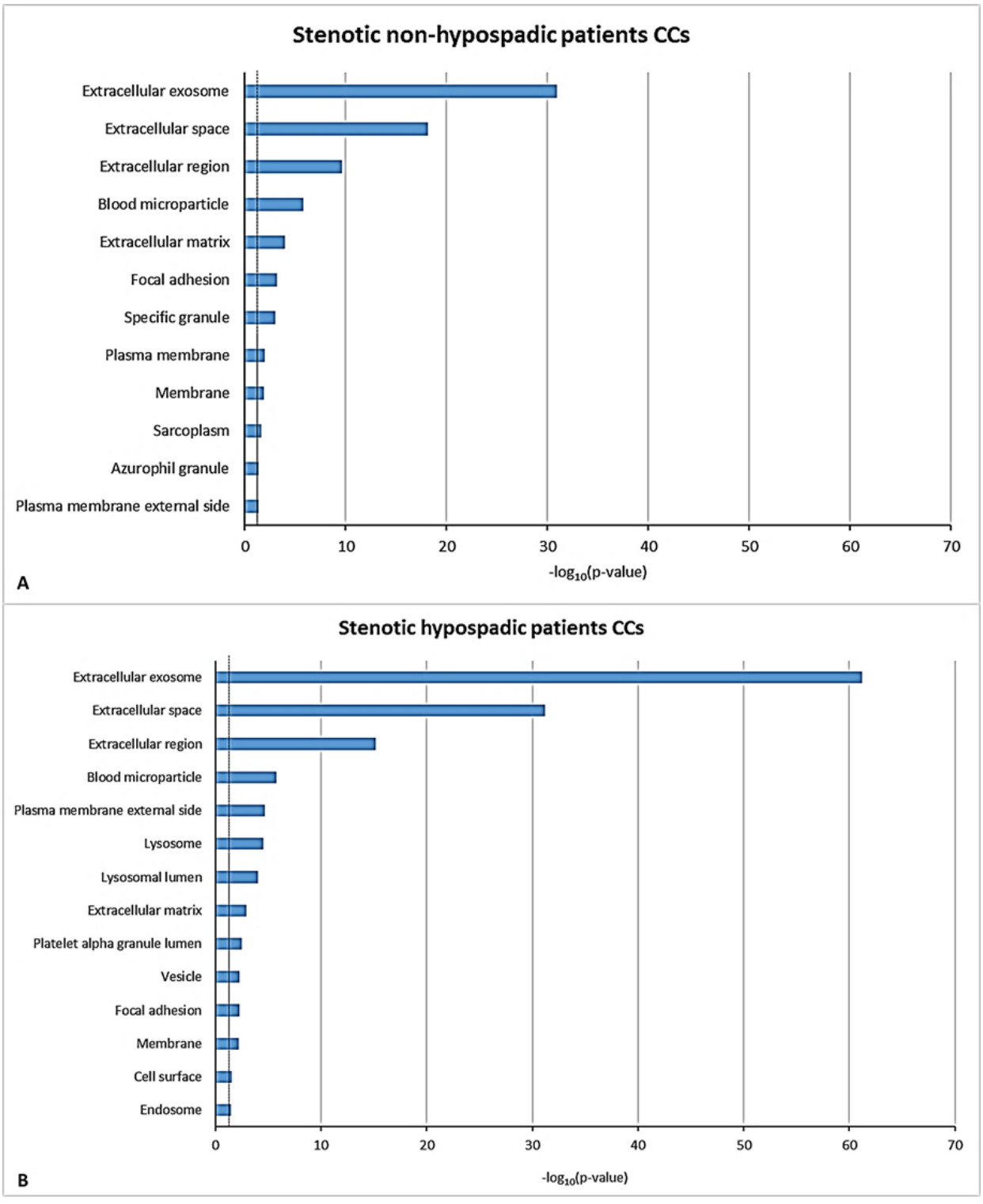

Figure 3.9. ***Cellular compartments represented in hypospadic (A) and non-hypospadic (B) urethral stricture patients.*** *Dashed black lines indicate the p-value threshold of 0.05.*

From the MF category, serine-type endopeptidase inhibitor activity, peptidoglycan receptor activity, and collagen binding were statistically significant in both type of patients (Fig.3.10). Interestingly, for non-hypospadic stenotic patients, calcium ion and laminin bindings are two of the most statistically significant represented MFs (Fig.3.10A). Peptidoglycan receptor activity, and small molecule and laminin bindings were the most enriched pathways for non-hypospadias patients, with a fold-enrichment of 107.18, 76.56, and 32.15, respectively.

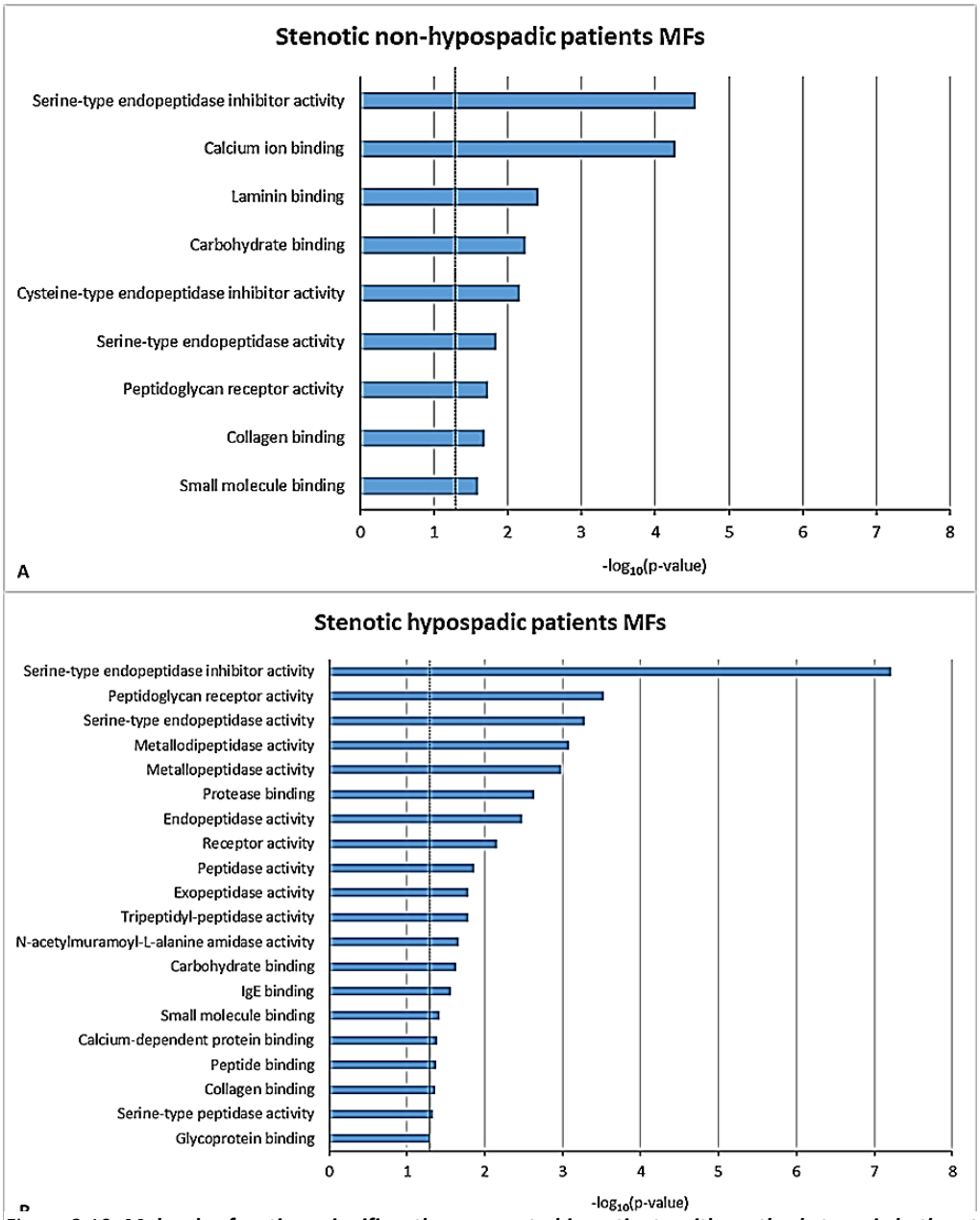

Figure 3.10. ***Molecular functions significantly represented in patients with urethral stenosis both not affected by hypospadias (A) or hypospadias affected (B).*** *Dashed black lines indicate the p-value threshold of 0.05.*

Protein association networks show associations between proteins that are significantly modulated in hypospadias (Fig.3.11A) and non-hypospadias urethral stricture patients (Fig.3.11B) compared to control. Line colors indicate the type of interaction evidence, both known interactions, such as from databases and experimentally determined, and predicted interactions, such as gene neighborhood, fusions, and co-occurrence.

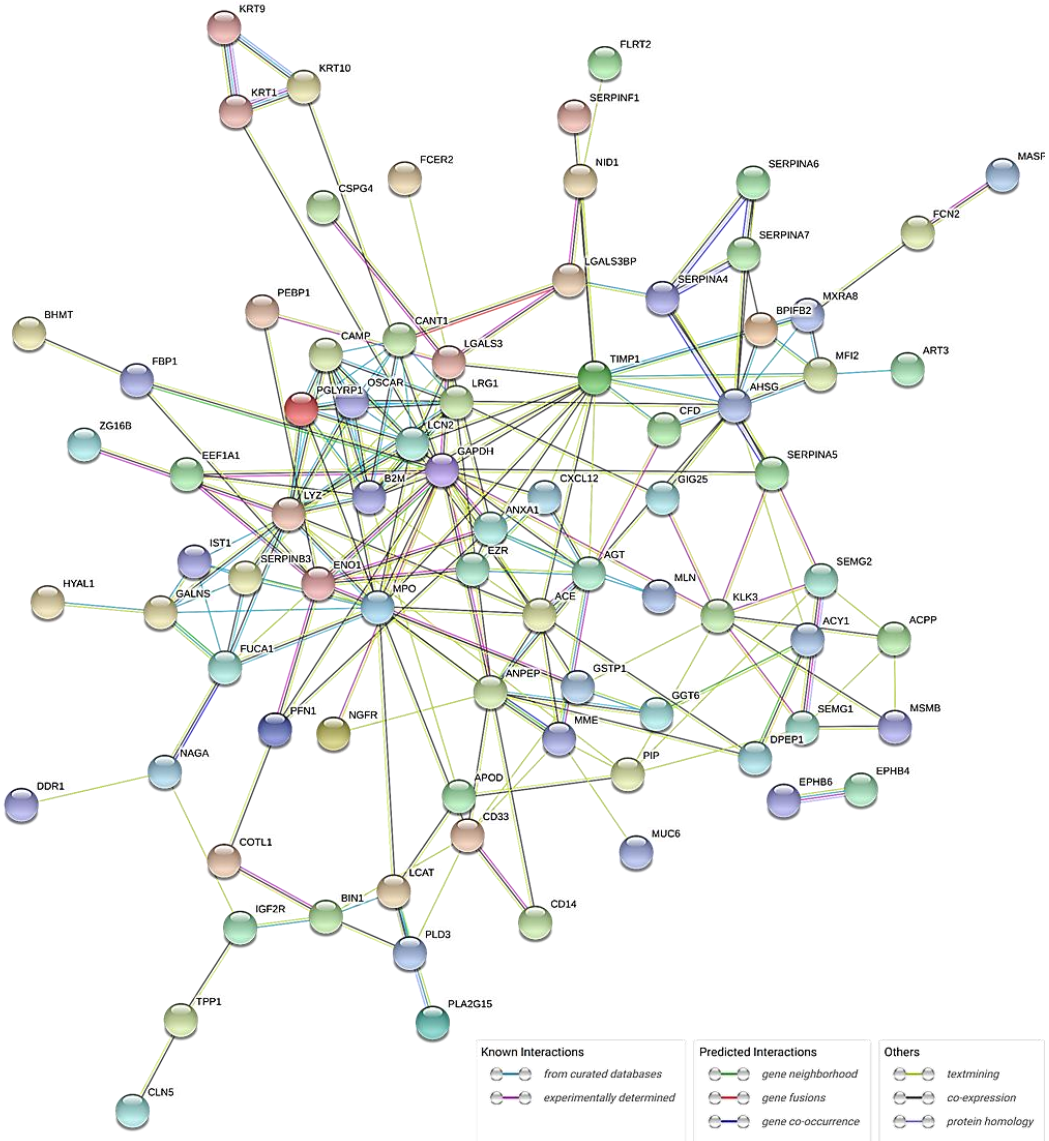

Figure 3.11A. ***Protein-protein interactions of urinary proteome in stenotic patients with hypospadias.***

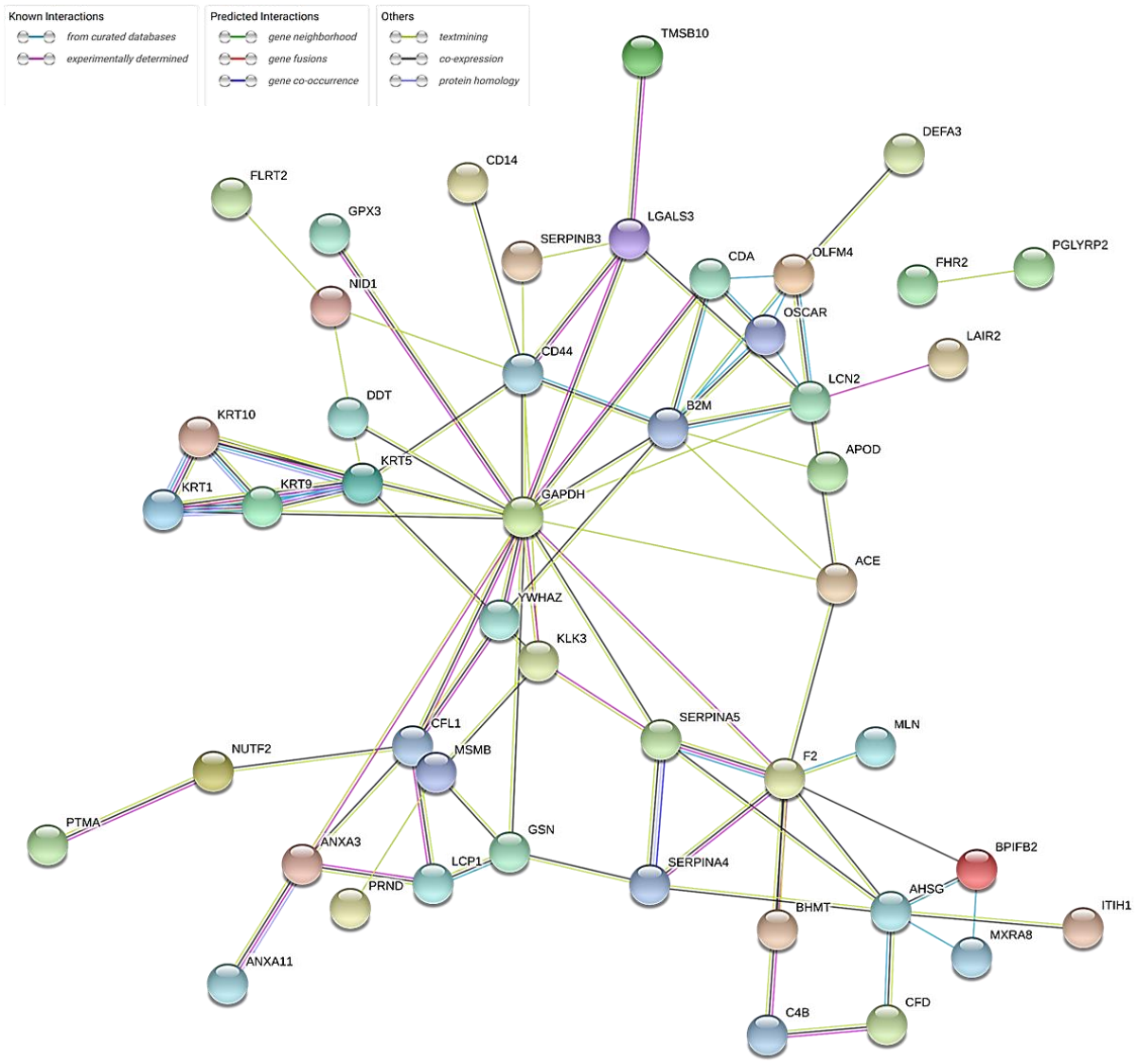

Figure 3.11B. ***Protein-protein interactions in urinary proteome of stenotic patients without hypospadias***

Interestingly, β_2 microglobulin (B2M), a protein involved in immune response regulation BPs, has been found to be downregulated in both hypospadic and non-hypospadic stenotic patients compared to control. However, its role is described as profibrotic in cardiac fibroblasts (Li *et al.*, 2018), in contrast with our finding in a fibrotic environment of the stricture disease locus; B2M is also the protein taking part in more BPs than any other GO-investigated protein: it is found to be involved in 11 BPs in hypospadias patients, and 5 in non-hypospadias stenotic patients; it is also involved in 7 CCs in non-hypospadic patients compared to control. Nidogen-1 (NID-1) also results downregulated in both type of patients compared to control. NID-1 has collagen- and laminin-

binding MFs, in fact it connects collagen- and laminin-formed networks to each other (Yurchenco & Patton, 2009), and it is involved in ECM disassembly and BM organization BPs, as it has roles in regenerating a structurally and functionally mature BM (Ponzi *et al.*, 2017). NID-1 is also the protein involved in more MF terms than any other, in the non-hypospadias group, being implicated in 3 MFs. Galectin-3, found absent in both type of patients, is an ECM cellular component with laminin-binding MF, which enhances fibrotic and inflammatory markers expression in cardiac fibroblasts (Arrieta *et al.*, 2019); moreover, it is upregulated in cases of liver, renal, and idiopathic pulmonary fibroses (IPF; Mackinnon *et al.*, 2012). Peptidoglycan recognition protein-2 (PGLYRP-2) is also downregulated in patients compared to control and is involved in inflammatory response regulation as well as IFNγ production negative regulation BPs; it has been found upregulated in fibrotic liver disease (Smalling *et al.*, 2013). Pigment epithelium-derived factor (PEDF) encoded by the gene *SERPINF1*, is absent in both type of patients, and as a matter of fact it contributes to healing wounds resolution by promoting a return to tissue homeostasis after injury (Wietecha *et al.*, 2015), it prevents liver fibrosis (Tsai *et al.*, 2014), and it has anti-oxidative and anti-fibrogenic properties (Mao *et al.*, 2011). Of note, keratin-1, an ECM CC, and keratin-9, have been found to be significantly modulated in all the comparisons: they are upregulated in non-hypospadic patients compared to hypospadic ones, and they are also found to be downregulated in the hypospadic group compared to the control. Keratin-9 has the highest positive FC (17.03) among all modulated proteins in non-hypospadias patients compared to control.

4. DISCUSSION

4.1. Oral mucosa as a substitute for urethral tissue

Severe hypospadias correction treatments involving urethral plate substitution can bring downsides. For example, surgeries employing skin flaps have a one-chance only to use foreskin and hair ingrowth risk. Indeed, the majority of urethroplasty surgeries exploit oral mucosal grafts. The autologous full-thickness oral mucosa tissue avoids complications as rejections due to histo-incompatibility. Problems occurred with this technique are difficulty in mouth opening, changes in salivary function (Markiewicz *et al.*, 2008), and oral contractures (Fasolis *et al*., 2014). Therefore, oral mucosal application for urethra reconstruction in hypospadias patients does not represent a long-term and conclusive solution. Since doubts remained about whether the heterotopic application of cultured cells can efficiently mimic urethral tissue or would instead result in adverse reactions, here was presented a protocol for oral mucosal stem cells cultivation and comparison with urethral culture; the epithelia intended for urethra replacement have been produced exploiting the epithelial stem cells regenerative capacities. In fact, regenerative medicine approaches offer innovative solutions for the treatment of diseases in which traditional medicine has limitations. The clinical application of this new investigational protocol can implicate adverse events and contamination; therefore we followed the guidelines regulating these advanced therapy medicinal products (ATMPs). Cell-based ATMPs are pharmaceuticals containing biological components and should be compliant with specific directives including Good Manufacturing Practice (GMP) and Good Clinical Practice (GCP) rules. We designed an ATMP for the repair of severe hypospadias treatment failure, to overcome major transplant challenges, such as the poor tissue collection possibilities (twice in total) and customizable graft size lack. Source material, as all steps of the process need an extended characterization for ATMP production, in this regulatory framework. Hence, in this study, oral mucosa was evaluated as a putative urethral substitute at cellular and molecular levels. Protein analysis revealed that keratin expression was comparable in both epithelia, with the exception for keratin-8 (K8) expressed in urethral cells only, both *in vitro* and paired with K18 *in vivo*. K8 and K18 expressions are known to be typical of pseudostratified epithelium as the urothelium (Alonso *et al.*, 2009), while K8 expression is typical of oral malignancies. Its negativity in the cultivated oral epithelium provides

reassurances as for malignancy absence. K8 plays a role in maintaining cellular structural integrity, perhaps its absence could be responsible for stricture occurrence after hypospadias surgery, but further investigations are required. The repression of Hox gene in oral mucosa holoclones was highlighted in transcriptome analysis of oral mucosa *vs.* urethral stem cells from **u**rethral **s**tricture **d**isease (USD) patients. Since Hox genes repression has been shown to preserve stem cell undifferentiated state (Biehs *et al.*, 2013), this finding is consistent with USD patient condition, and a stemness loss could originate from the pathology. After assessment of the advantages of oral mucosa epithelium over diseased urethra for tissue reconstruction, no significant differences were noted between the two epithelia, suggesting oral mucosa as a valid substitute for urethral tissue.

4.2. Drug product manufacturing and administration

Efficient production of functional oral mucosal epithelia was possible with GMP-validated methods, along with safety evaluation and quality control assays standards, confirming the suitability for clinical translation. Epithelial stem cells maintenance is very important for the cultured tissue to engraft and persist, to long-term self-renew, and to restore missing functionality (Rama *et al.*, 2010). Indeed, stem cell maintenance was proven in cultivated oral mucosal keratinocytes. BMI-1 and p63 are two possible potency markers for epithelial stem cell identification. They are, in fact, related to the long-term capacity for proliferation and self-renewal in several cell types (Barbaro *et al.*, 2007; Molofsky *et al.*, 2005). Oral mucosa stem cell clones presented higher BMI-1 and p63 levels than transient amplifying (TA) clones, and their expression progressively decreased with replicative senescence and differentiation (Corradini *et al.*, 2016). Moreover, *TP63* KO mice revealed stratified squamous epithelial linings disappearance including urethral and prostatic tissue (Yang *et al.*, 1999; Senoo *et al.*, 2007). BMI-1 mediates oral mucosa lifespan extension and can repress *CDKN2A*-encoded cell-cycle inhibitors p16 and p14ARF (Biehs *et al.*, 2013). In addition, BMI-1 downregulation was shown to suppress cancer stem cell functions (Srinivasan *et al.*, 2017). However, it still needs to be demonstrated whether other mechanisms determining stemness potency are in place in this area. Correlation studies are still required to fully define the optimal potency assay specification limits, as at early stages of clinical trials the product potency cannot be fully determined. The optimal specification limits

for purity assays and the follow-up investigations should also be updated at the end of clinical trials. Nonetheless, the protocol promotes a remarkable cell expansion from a very small biopsy, maintaining reproducibility and scalability. Nowadays, the nonclinical testing strategy should comply with the 2009/120/EC Commission Directive, listing requirements on the pharmacological and toxicological medicinal products testing. Indeed, the standard approach may not always be applicable due to the distinctive and varied ATMP structural and biological properties. Consequently, nonclinical *in vivo* animal-based testing was not performed, following also the Three Rs guiding principles on animal testing: ***R***eplacement of animal use in research, ***R***eduction of animal numbers used per experiment, and ***R***efinement of methods to minimize animal suffering and improve welfare. Moreover, *in vitro* animal models showed very significant inconsistencies in comparison with human cell behaviors under the selected culture conditions. Biological knowledge together with surgical expertise allowed an efficient manufacturing process implementation and a standardized clinical protocol definition for drug product (DP) administration. The combination of oral mucosal cells between a biocompatible double fibrin scaffold in a tissue-engineered construct, ensures rapid and continuous epithelium adhesion, preserving the epithelial proliferative potential from damages due to transportation, surgical handling and post-operative maneuvers. The fibrin is a physiological wound healing substrate and fibrin matrices with appropriate thickness, mechanical strength, and flexibility are rapidly reabsorbed upon administration, allowing epithelium engraftment and therapeutic effects (Rama *et al.*, 2001; Macasev *et al.*, 2011; Sese *et al.*, 2011). The DP formulation is designed to ensure cell viability maintenance over its shelf life, as this construct was proven to provide a normal stratified epithelium populated by the long-living tissue stem cells, granting a potent and viable DP. This specific construct provides also resistance and protection during transport and surgical handling. The hypothetic therapeutic action mechanism involves missing section replacement by the oral mucosa epithelium: after graft adhesion as a result of fibrin degradation, oral mucosa cells would proliferate and differentiate for tissue repair, producing also factors for paracrine stimulation on the surrounding environment. The assessment of 1-year follow-up data on product safety and treatment efficacy can confirm the long-term treatment stability. These

combined data will support the understanding and the safety of the proposed treatment for urethra restoration to address this medical need.

4.3. Urinary proteome characterization: a pilot study

Hypospadias retreatment after previous surgery failure requires a delicate procedure and implicates variable positive and negative outcomes (Barbagli *et al.*, 2010). The presence of fibrotic tissue, strictures and scarring is responsible for the inflammatory environment and endangers the therapeutic success. The optimal surgery condition would be pediatric patient primary treatment, allowing epithelium adhesion on a scar-free site with a physiologic inflammation process. Since now it is not possible to identify non-responsive patients in hypospadias surgery treatment, urinary biomarker proteomics investigations described secretory proteins possibly implicated in urethral fibrosis. USD, one of the main complications after failed hypospadias treatment, is in fact characterized by lumen reduction and lining scarring (Santucci *et al.*, 2007). Growth factors and cytokines initiating the inflammatory cascade following injury are directly linked to the extent of scar formation (Eming *et al.*, 2007), influencing fibroblast proliferation and collagen metabolism (Seo *et al.*, 1996), responsible for enhanced extracellular matrix (ECM) deposition, thanks to fibronectin and proteoglycans productions. These are required to build the new connective tissue matrix but are also associated with pathological proliferative conditions characterized by fibrosis, such as Peyronie's disease (Sappino *et al.*, 1990). Most nonhealing wounds fail to progress through the normal wound repair phases and remain in a chronic inflammatory state (Loots *et al.*, 1998). Therefore, excessive growth factor secretion and the lack of molecules required for apoptosis or ECM remodeling might produce scarring processes (Nauta *et al.*, 2011). Mass spectrometry analysis revealed downregulation of most of the secreted modulated proteins in USD patients compared to control, indicating that inhibitory processes for protein secretion are prevalent in respect to stimulatory ones in patients. Type II K1 is physiologically expressed in the epidermis most differentiated layers, and it is usually paired with family member type I K10. It plays a role in epidermal barrier establishment on plantar skin (Fischer *et al.*, 2016), and therefore it also is expressed in a terminally differentiated state. Also K9 physiologically serves functions in the mature plantar skin tissue, as well as in the palmar one (Langbein *et al.*, 1993). These keratins were downregulated in hypospadic USD

patients while upregulated in non-hypospadic ones. This may indicate an advanced differentiated state of the damaged epithelium in the non-hypospadic patients, while its lower levels in hypospadic patients is reminiscent of their condition in which the epithelium is absent. Moreover, cultivated urethral keratinocytes deriving from non-hypospadic USD patients display a lower cell doubling number (Corradini *et al*., 2016) compared to healthy urethral keratinocytes (Sceberras *et al.*, 2019), correlating with their tendency to differentiate sooner. Nidogen-1 (NID-1) is an essential sulfated glycoprotein component of the basement membrane (BM). BM regeneration after injury occurs by a self-assembly process in which laminins bind to other laminin and cell surface molecules. The laminin scaffold enables BM components recruitment and assembly, including NID-1, to regenerate the structurally and functionally mature BM (Ponzi *et al.*, 2017). NID-1 connects collagen IV- and laminin-formed networks to each other (Yurchenco & Patton, 2009). NID-1 has indeed been demonstrated to have roles in building a functional BM in decellularized tissue scaffolds derived from subpleural idiopathic pulmonary fibrosis (IPF) lungs (Elowsson Rendin *et al.*, 2019). Therefore, it can be speculated that BM disorganization and irregular formation could be favored if NID-1 is downregulated as in USD patients. This is also the case in Sjögren's syndrome patients, where the labial salivary glands basal lamina is disorganized in association with nidogen fragment degradation elevation (Kwon *et al.*, 2006). β_2 microglobulin (B2M) has a profibrotic role in cardiac fibroblasts (Li *et al.*, 2018), and B2M blood levels are found to be increased in rat models affected by renal interstitial fibrosis (RIF; Zheng *et al.*, 2018). B2M in urethral stricture patients has an opposite behavior in what is observed in cultivated cardiac fibroblasts or RIF rat models, and it can be speculated that since scar tissue is generally functionally less efficient (Xue & Jackson, 2015), B2M is not implicated in urethral fibrosis possibly due to impaired secretion from the damaged and densely scarred urethral lumen of USD patients. Peptidoglycan recognition protein family members are implicated in inflammatory responses: peptidoglycan recognition protein-2 (PGLYRP-2) KO mice are found to be resistant to peptidoglycan-induced arthritis and local inflammation (Saha *et al.*, 2009). However, they are also more sensitive to experimental psoriasis-like inflammation development, because PGLYRP-2 limits T helper 17 cells overactivation by promoting regulatory T cells accumulation at the inflammation site, protecting the skin from exaggerated inflammatory responses (Park *et al.*,

2011). In humans, PGLYRP-2 has been found upregulated in liver specimens of patients with fibrotic liver disease (Smalling *et al.*, 2013). Due to PGLYRP-2 dual inflammatory role in mice, and its opposite trend to what is observed in other type of human fibroses, further investigations are required. Pigment epithelium-derived factor (PEDF) has functional variety including antiangiogenic, antitumorigenic, and neurotrophic properties (Rychli *et al.*, 2009). PEDF is known to contribute to healing wounds resolution by promoting a return to tissue homeostasis after injury (Wietecha *et al.*, 2015), to prevent liver fibrosis (Tsai *et al.*, 2014), to act as a compensatory antifibrotic cytokine in pancreatitis (Schmitz *et al.*, 2011), and to have anti-oxidative and anti-fibrogenic properties in cultured human glomerular mesangial cells (Mao *et al.*, 2011), In accordance with its absence in the inflamed and fibrotic environment of the urethral lumen. These results give a preliminary description of USD patient urinary proteome. However, one of the limits of this investigation was the limited sample number and the fact that to increase detectable protein content it was necessary to pool together urine samples. Despite USD patients can be classified depending on where the stricture localizes, patients can be very heterogeneous as a population and somewhat difficult to categorize, and this can add biases to the analysis. Lastly, the urine proteome can be representative of all the urinary tract starting from renal glomerulus and could be descriptive of the entire organism inflammatory state. Nonetheless, differentially expressed proteins (DEPs) functional enrichment analysis highlighted BM organization as a significantly represented biological process in USD patients, indicating an accurate clinical feature description. Also innate immune response was statistically significant in patients, consistent with the USD patient pathology, as patients are highly susceptible to urethral infections. Moreover, response to reactive oxygen species, inflammatory response, and cytokine secretion were represented, indicating an altered inflammatory status presence, in accordance with the clinical features of the pathology. Specialized tissue-resident natural killer (NK) cell subset populations play a role in organ homeostasis (Sojka *et al.*, 2014). For example, NK cells with a specific phenotype are enriched in the human liver (Hudspeth *et al.*, 2016) and limit liver fibrosis by killing hepatic stellate cell-derived myofibroblasts, which play a key role in the pathogenic process (Fasbender *et al.*, 2016). Negative regulation of NK cell differentiation involved in immune response is taking place in recurrent-stenotic hypospadic patients, and it can

be speculated that this biological process is not taking place in these patients, possibly explaining the non-resolution of fibrosis, but further investigations are required. Collagen and laminin bindings in USD patients possibly indicate that ECM and BM formations are taking place in repair attempts from the body. In the immediate future urinary proteome changes will be studied in the same patients investigated in this study, so to eliminate inter-patient variability. Patients will be clinically assessed both as treatment successes and failures every 12 months. Possibly, in the future, a larger cohort of patients will be analyzed, as to increment statistical relevance. Once the markers will be identified, specific assays aimed at determining urinary markers levels will be designed. ELISA can be a valuable option, as it was already employed to analyze urinary changes in idiopathic nephrotic syndrome (Woroniecki *et al.*, 2008) or Henoch-Schönlein purpura patients (Chen *et al.*, 2014). Other future approaches may include macrophage analysis. In fact, a switch failure from a proinflammatory M1 to an anti-inflammatory M2 phenotype leads to increased inflammation and increased TNF proteins secretion (Hesketh *et al.*, 2017). Moreover, if M2 activity is left unchecked, M2 macrophages produce large TGF-β1 amounts, promoting excessive myofibroblast formation and subsequent excessive collagen production and ECM deposition, leading to fibrosis (Mahdavian Delavary *et al.*, 2011).

In conclusion, thanks to keratinocyte stem cell culture advances, a tissue engineered ATMP was developed to be used in urethral reconstruction, reducing complications and morbidity at donor and receiving sites. Patient urinary proteome description can aid at therapy improvement to select non-responsive patients with further treatment required and enhancing success outcomes after USD therapy.

REFERENCES

Adams D. Keratinization of the oral epithelium. Ann R Coll Surg Engl. 1976 Sep;58(5):351-8. Review.

Alonso A, Ikinger U, Kartenbeck J. “Staining patterns of keratins in the human urinary tract.” Histol Histopathol. 2009 Nov;24(11):1425-37.

Andersson, M., Doroszkiewicz, M., Arfwidsson, C., Abrahamsson, K. & Holmdahl, G. Hypospadias repair with tubularized incised plate: does the obstructive flow pattern resolve spontaneously? J. Pediatr. Urol. 7, 441–445 (2011)

Anson ML (1940). "The reactions of Iodine and Iodoacetamide with native Egg Albumin". J. Gen. Physiol. 23 (3): 321–31.

Arrieta V, Sádaba JR, Álvarez V, Rodríguez JA, López-Andrés N. “Galectin-3 as a novel biotarget in cardiovascular alterations associated to development of severe aortic stenosis.” An Sist Sanit Navar. 2019 Aug 23;42(2):199-208

Barbagli G, De Angelis M, Palminteri E et al: Failed hypospadias repair presenting in adults. Eur Urol 2006; 49: 887

Barbagli G, Perovic S, Djinovic R, Sansalone S, Lazzeri M. Retrospective descriptive analysis of 1176 patients with failed hypospadias repair. J Urol 2010; 183: 207–11

Barbaro V, Testa A, Di Iorio E, Mavilio F, Pellegrini G, De Luca M (2007) C/EBPdelta regulates cell cycle and self-renewal of human limbal stem cells. J Cell Biol 177(6):1037–1049

Barrandon and Green 1987, Three Clonal types of keratinocyte with different capacities for multiplication. Proc Natl Acad Sci US 1987 Apr; 84(8):2302-6.

Barrandon Y, Green H. Cell size as a determinant of the clone-forming ability of human keratinocytes. Proc Natl Acad Sci U S A. 1985 Aug;82(16):5390-4.

Baskin et al., Hypospadias: anatomy, etiology, and technique. Journal of Pediatric Surgery, 2006, 41, 463-472

Bergman JE, Loane M, Vrijheid M, Pierini A, Nijman RJ, Addor MC, Barisic I, Béres J, Braz P, Budd J, Delaney V, Gatt M, Khoshnood B, Klungsøyr K, Martos C, Mullaney C, Nelen V, Neville AJ, O'Mahony M, Queisser-Luft A, Randrianaivo H, Rissmann A, Rounding C, Tucker D, Wellesley D, Zymak-Zakutnia N, Bakker MK, de Walle HE. Epidemiology of hypospadias in Europe: a registry-based study. World J Urol. 2015 Dec;33(12):2159-67

Biehs B, Hu JK, Strauli NB, Sangiorgi E, Jung H, Heber RP, Ho S, Goodwin AF, Dasen JS, Capecchi MR, Klein OD (2013) BMI1 represses Ink4a/Arf and Hox genes to regulate stem cells in the rodent incisor. Nat Cell Biol 15(7):846–852

Caubet C, Lacroix C, Decramer S, Drube J, Ehrich JH, Mischak H, et al. Advances in urinary proteome analysis and biomarker discovery in pediatric renal disease. Pediatr Nephrol 2009; 25: 27–35.

Chen CL, Lai YF, Tang P, Chien KY, Yu JS, Tsai CH, et al. Comparative and targeted proteomic analyses of urinary microparticles from bladder cancer and hernia patients. J Proteome Res 2012; 11: 5611–29.

Chen CL, Lin TS, Tsai CH, Wu CC, Chung T, Chien KY, Wu M, Chang YS, Yu JS, Chen YT. “Identification of potential bladder cancer markers in urine by abundant-protein depletion coupled with quantitative proteomics.” J Proteomics. 2013 Jun 24; 85: 28-43.

Chen T, Lu YH, Wang WJ, Bian CY, Cheng XY, Su Y, Zhou PM. Elevated urinary levels of cystatin C and neutrophil gelatinase-associated lipocalin in Henoch-Schönlein purpura patients with renal involvement. PLoS One. 2014 Jun 25;9(6): e101026

Corradini F, Zattoni M, Barbagli G Et al. Comparative Assessment of Cultures from Oral and Urethral Stem Cells for Urethral Regeneration. Curr Stem Cell Res Ther. 2016; 11(8):643-651.

Culp OS, McRoberts JW: Hypospadias. In Alken CE, Dix VW, Goodwin WE, et al, Encyclopedia of Urology, New York, Springer 1968: 11: 307-344

de Kemp V, de Graaf P, Fledderus JO, Ruud Bosch JL, de Kort LM. Tissue engineering for human urethral reconstruction: systematic review of recent literature. PLoS One. 2015 Feb 17;10(2):e0118653

De Luca M, Pellegrini G, Green H. Regeneration of squamous epithelia from stem cells of cultured grafts. Regen Med. 2006 Jan;1(1):45-57. Review.

Dellambra E, Golisano O, Bondanza S, Siviero E, Lacal P, Molinari M, D'Atri S, De Luca M. Downregulation of 14-3-3sigma prevents clonal evolution and leads to immortalization of primary human keratinocytes. J Cell Biol. 2000 May 29;149(5):1117-30.

El-Kassaby AW1, El-Zayat TM, Azazy S, Osman T. One-stage repair of long bulbar urethral strictures using augmented Russell dorsal strip anastomosis: outcome of 234 cases. Eur Urol. 2008 Feb;53(2):420-4.

Elowsson Rendin L, Löfdahl A, Åhrman E, Müller C, Notermans T, Michaliková B, Rosmark O, Zhou XH, Dellgren G, Silverborn M, Bjermer L, Malmström A, Larsson-Callerfelt AK, Isaksson H, Malmström J, Westergren-Thorsson G. “Matrisome Properties of Scaffolds Direct Fibroblasts in Idiopathic Pulmonary Fibrosis.” Int J Mol Sci. 2019 Aug 17;20(16). pii: E4013

Eming SA, Krieg T, Davidson JM: Inflammation in wound repair: molecular and cellular mechanisms. J Invest Dermatol 2007; 127: 514–525

Fasbender F, Widera A, Hengstler JG, Watzl C (2016). "Natural Killer Cells and Liver Fibrosis". Frontiers in Immunology. 7: 19.

Fasolis M, Zavattero E, Sedigh O, Gontero P, Preto M, Frea B, Ramieri G. Oral Mucosa harvest for urologic reconstruction: role of maxillofacial surgeon and donor-site morbidity evaluation. J Craniofac Surg. 2014 Mar; 25(2):604-6.

Fischer H., Langbein L., Reichelt J., Buchberger M., Tschachler E., Eckhart L. "Keratins K2 and K10 are essential for the epidermal integrity of plantar skin." J. Dermatol. Sci. 81:10-16 (2016)

Fisher WG, Lucas JE, Mehdi UF, Qunibi DW, Garner HR, Rosenblatt KP, Toto RD. A method for isolation and identification of urinary biomarkers in patients with diabetic nephropathy. Proteomics Clin Appl. 2011 Dec;5(11-12):603-12.

Fossati, N., Barbagli, G., Larcher, A., Dell'Oglio, P., Sansalone, S., Lughezzani, G., … Lazzeri, M. (2016). The surgical learning curve for one-stage anterior urethroplasty: A prospective single-surgeon study. European Urology, 69(4), 686–690.

Gatti JM, Krisch A, Snyder HM III: Hypospadias. eMedicine CME 2003;1–13

Gonzalez LM, Moeser AJ, Blikslager AT (2015) Porcine models of digestive disease: the future of large animal translational research. Transl Res 166 (1):12-27.

Good D. M., V. Thongboonkerd, J. Novak et al., “Body fluid proteomics for biomarker discovery: lessons from the past hold the key to success in the future,” Journal of Proteome Research, vol. 6, no. 12, pp. 4549–4555, 2007.

Green H, Kehinde O, Thomas J “Growth of cultured human epidermal cells into multiple epithelia suitable for grafting.” Proc Natl Acad Sci US 1979 Nov; 76 (11): 5665-8.

Grimsby GM, Baker LA. The Use of autologous buccal mucosa grafts in vaginal reconstruction. Curr Urol Rep. 2014 Aug; 15(8):428.

Groenen MA, Archibald AL, Uenishi H, Tuggle CK, Takeuchi Y, Rothschild MF, Rogel-Gaillard C, Park C, Milan D, Megens HJ, Li S, Larkin DM, Kim H, Frantz LA, Caccamo M, Ahn H, Aken BL, Anselmo A, Anthon C, Auvil L, Badaoui B, Beattie CW, Bendixen C, Berman D, Blecha F, Blomberg J, Bolund L, Bosse M, Botti S, Bujie Z, Bystrom M, Capitanu B, Carvalho-Silva D, Chardon P, Chen C, Cheng R, Choi SH, Chow W, Clark RC, Clee C, Crooijmans RP, Dawson HD, Dehais P, De Sapio F, Dibbits B, Drou N, Du ZQ, Eversole K, Fadista J, Fairley S, Faraut T, Faulkner GJ, Fowler KE, Fredholm M, Fritz E, Gilbert JG, Giuffra E, Gorodkin J, Griffin DK, Harrow JL, Hayward A, Howe K, Hu ZL, Humphray SJ, Hunt T, Hornshoj H, Jeon JT, Jern P, Jones M, Jurka J, Kanamori H, Kapetanovic R, Kim J, Kim JH, Kim KW, Kim TH, Larson G, Lee K, Lee KT, Leggett R, Lewin HA, Li Y, Liu W, Loveland JE, Lu Y, Lunney JK, Ma J, Madsen O, Mann K, Matthews L, McLaren S, Morozumi T, Murtaugh MP, Narayan J, Nguyen DT, Ni P, Oh SJ, Onteru S, Panitz F, Park EW, Park HS, Pascal G, Paudel Y, Perez-Enciso M, Ramirez-Gonzalez R, Reecy JM, Rodriguez-Zas S, Rohrer GA, Rund L, Sang Y, Schachtschneider K, Schraiber JG, Schwartz J, Scobie L, Scott C, Searle S, Servin B, Southey BR, Sperber G, Stadler P, Sweedler JV, Tafer H, Thomsen B, Wali R, Wang J, Wang J, White S, Xu X, Yerle M, Zhang G, Zhang J, Zhang J, Zhao S, Rogers J, Churcher C, Schook LB (2012) Analyses of pig genomes provide insight into porcine demography and evolution. Nature 491 (7424):393-398.

Gürdal M, Tekin A, et al. Intermediate-term functional and cosmetic results of the Snodgrass procedure in distal and midpenile hypospadias. Pediatr Surg Int 2004; 20: 197-199

Hampson, L. A., McAninch, J. W., & Breyer, B. N. (2014). Male urethral strictures and their management. Nature Reviews Urology, 11(1), 43–50.

Hesketh M, Sahin KB, West ZE, Murray RZ (July 2017). "Macrophage Phenotypes Regulate Scar Formation and Chronic Wound Healing". International Journal of Molecular Sciences. 18 (7): 1545

Hofer MD, Cheng EY, Bury MI, Park E, Xu W, Hong SJ, Kaplan WE, Sharma AK. Analysis of primary urethral wound healing in the rat. Urology. 2014; 84 (1): 246

Huang da W, Sherman BT, Lempicki RA. 2009. Systematic and integrative analysis of large gene lists using DAVID bioinformatics resources. Nature Protocols 4:44-57

Huang, S., Yang, C., Li, M., Wang, B., Chen, H., Fu, D., & Chong, T. (2018). Effect of dual mTOR inhibitor on TGFbeta1-induced fibrosis in primary human urethral scar fibroblasts. Biomedicine & Pharmacotherapy, 106, 1182–1187.

Hudspeth K, Donadon M, Cimino M, Pontarini E, Tentorio P, Preti M, Hong M, Bertoletti A, Bicciato S, Invernizzi P, Lugli E, Torzilli G, Gershwin ME, Mavilio D (January 2016). "Human liver-resident CD56(bright)/CD16(neg) NK cells are retained within hepatic sinusoids via the engagement of CCR5 and CXCR6 pathways". Journal of Autoimmunity. 66: 40–50.

Isono K, Mizutani-Koseki Y, Komori T, Schmidt-Zachmann MS, Koseki H (2005) Mammalian polycomb-mediated repression of Hox genes requires the essential spliceosomal protein Sf3b1. Genes Dev 19(5):536–541

Janech M. G., J. R. Raymond, and J. M. Arthur, “Proteomics in renal research,” The American Journal of Physiology—Renal Physiology, vol. 292, no. 2, pp. F501–F512, 2007.

Jones KB, Klein OD. Oral epithelial stem cells in tissue maintenance and disease: the first steps in a long journey. Int J Oral Sci. 2013 Sep;5(3):121-9.

Kallen B, Bertollini R, Castilla E, et al.: A joint international study on the epidemiology of hypospadias. Acta Paediatr Scand Suppl. 1986; 324:1-52

Kushnir MM, Mrozinski P, Rockwood AL, Crockett DK. A depletion strategy for improved detection of human proteins from urine. J Biomol Tech 2009; 20: 101–8.

Kwon YJ, Pérez P, Aguilera S, Molina C, Leyton L, Alliende C, Leyton C, Brito M, Romo R, González MJ. “Involvement of specific laminins and nidogens in the active remodeling of the basal lamina of labial salivary glands from patients with Sjögren's syndrome.” Arthritis Rheum. 2006 Nov;54(11):3465-75

Langbein L., Heid H.W., Moll I., Franke W.W. "Molecular characterization of the body site-specific human epidermal cytokeratin 9: cDNA cloning, amino acid sequence, and tissue specificity of gene expression." Differentiation 55:57-72(1993)

Li Y, Zhang X, Li L, Wang X, Chen Z, Wang X, Wang Y, Kang L, Ye Y, Jia J, Zhang G, Yang C, Yuan J, Zhou J, Ge J, Gong H, Zou Y. “Mechanical stresses induce paracrine β-2 microglobulin from cardiomyocytes to activate cardiac fibroblasts through epidermal growth factor receptor” Clin Sci (Lond). 2018 Aug 30;132(16):1855-1874

Li Z, Chen P, Su R, Hu C, Li Y, Elkahloun AG, Zuo Z, Gurbuxani S, Arnovitz S, Weng H, Wang Y, Li S, Huang H, Neilly MB, Wang GG, Jiang X, Liu PP, Jin J, Chen J (2016) PBX3 and MEIS1 cooperate in hematopoietic cells to drive acute myeloid leukemias characterized by a core transcriptome of the MLL-rearranged disease. Cancer Res 76(3):619–629

Liu Z., Z. Yuan, and Q. Zhao, “SELDI-TOF-MS proteomic profiling of serum, urine, and amniotic fluid in neural tube defects,” PLoS ONE, vol. 9, no. 7, Article ID e103276, 2014.

Loots MA, Lamme EN, Zeegelaar J, Mekkes JR, Bos JD, Middelkoop E: Differences in cellular infiltrate and extracellular matrix of chronic diabetic and venous ulcers versus acute wounds. J Invest Dermatol 1998; 111: 850–857

Lumen N, Hoebeke P, Willemsen P, et al. Etiology of urethral stricture disease in the 21st century. J Urol. 2009; 182: 983–987

Macasev D, Diorio JP, Gugerell A, Goppelt A, Gulle H, Bittner M. J Biomater Appl. Cell Compatibility of fibrin sealants: in vitro study with cells involved in soft tissue repair.2011 Aug; 26(2):129-49

Mackinnon AC, Gibbons MA, Farnworth SL, Leffler H, Nilsson UJ, Delaine T, Simpson AJ, Forbes SJ, Hirani N, Gauldie J, Sethi T (March 2012). "Regulation of transforming growth factor-β1-driven lung fibrosis by galectin-3". American Journal of Respiratory and Critical Care Medicine. 185 (5): 537–46

Mahdavian Delavary B, van der Veer WM, van Egmond M, Niessen FB, Beelen RH. Macrophages in skin injury and repair. Immunobiology. 2011; 216: 753-62

Manzoni G, Bracka A, Palminteri E, Marrocco G. Hypospadias surgery: when, what and by whom? BJU Int. 2004 Nov; 94(8):1188-95.

Mao T, Gao L, Li H, Li J. “Pigment epithelium-derived factor inhibits high glucose induced oxidative stress and fibrosis of cultured human glomerular mesangial cells.” Saudi Med J. 2011 Aug;32(8):769-77

Markiewicz MR, DeSantis JL, Margarone JE 3rd, Pogrel MA, Chuang SK. Morbidity Associated with oral mucosa harvest for urological reconstruction: an overview. J Oral Maxillofac Surg. 2008Apr; 66(4):739-44.

Moll R, Divo M, Langbein L. The human keratins: biology and pathology. Histochem Cell Biol. 2008 Jun;129(6):705-33. 2008 May 7. Review

Molofsky AV, He S, Bydon M, Morrison SJ, Pardal R (2005) Bmi-1 promotes neural stem cell self-renewal and neural development but not mouse growth and survival by repressing the p16Ink4a and p19Arf senescence pathways. Genes Dev 19(12):1432–1437.

Mouriquand PDE, Mure PY: Hypospadias. In: Gearhart JP, Mouriquand PDE, Rink R (eds) Pediatric urology. Saunders, Philadelphia, pp 713-728; 2001

Nauta A, Gurtner G, Longaker M: Wound healing and regenerative strategies. Oral Dis 2011 18; 17: 541–549

Neverova I, Van Eyk JE. "Role of chromatographic techniques in proteomic analysis." J Chromatogr B Analyt Technol Biomed Life Sci. 2005 Feb 5;815(1-2):51-63.

Niwa T., "Biomarker discovery for kidney diseases by mass spectrometry," Journal of Chromatography B, vol. 870, no. 2, pp. 148–153, 2008.

O' Connor NE, Mulliken JB, Green H. Grafting of burns with cultured epithelium prepared from autologous epidermal cells. Lancet. 1981 Jan 10; 1(8211):75-8.

Park SY, Gupta D, Hurwich R, Kim CH, Dziarski R. "Peptidoglycan recognition protein Pglyrp2 protects mice from psoriasis-like skin inflammation by promoting regulatory T cells and limiting Th17 responses." J Immunol. 2011 Dec 1;187(11):5813-23

Paulozzi LJ, Erickson JD, Jackson RJ. Hypospadias trends in two US surveillance systems. Pediatrics. 1997; 100: 831-834.

Pellegrini G, Golisano O, Paterna P, Lambiase A, Bonini S, Rama P, De Luca M. Location And clonal analysis of stem cells and their differentiated progeny in the human ocular surface. J Cell Biol. 1999 May 17; 145(4):769-82.

Perry BJ, Zammit AP, Lewandowski AW, Bashford JJ, Dragovic AS, Perry EJ, Hayatbakhsh R Perry CF. Sites Of origin of oral cavity cancer in non-smokers vs smokers: possible evidence of dental trauma carcinogenesis and its importance Compared with human papillomavirus. JAMA Otolaryngol Head Neck Surg. 2015 Jan; 141(1):5---11.

Pisitkun, T.; Johnstone, R.; Knepper, M. A. Mol. Cell. Proteomics 2006, 5, 1760−71.

Ponzi A, Yurchenco PD, Iozzo RV. The nature and biology of basement membranes. Matrix Biol. 2017; 57-58:1–11

Prakash M, Shetty JK, Dash S, Barik BK, Sarkar A, Prabhu R. "Determination of urinary peptides in patients with proteinuria." Indian J Nephrol. 2008 Oct;18(4):150-4.

Rama P, Bonini S, Lambiase A, Golisano O, Paterna P, De Luca M, Pellegrini G. Autologous fibrin-cultured limbal stem cells permanently restore the corneal surface of patients with total limbal stem cell deficiency. Transplantation. 2001 Nov 15; 72(9):1478-85

Ram-Liebig G, Barbagli G, Heidenreich A, Fahlenkamp D, Romano G, Rebmann U, Standhaft D, van Ahlen H, Schakaki S, Balsmeyer U, Spiegler M, Knispel H. Results of Use of Tissue-Engineered Autologous Oral Mucosa Graft for Urethral Reconstruction: A Multicenter, Prospective, Observational Trial. EBioMedicine. 2017 Sep; 23: 185-192.

Romagnoli G, De Luca M, Faranda F, Bandelloni R, Franzi AT, Cataliotti F, Cancedda R. Treatment Of posterior hypospadias by the autologous graft of cultured urethral epithelium. N Engl J Med. 1990 Aug 23; 323(8):527-30.

Romagnoli G, De Luca M, Faranda F,Franzi AT, Cancedda R. One-step Treatment of proximal hypospadias by the autologous graft of cultured urethral epithelium. J Urol. 1993 Oct; 150(4):1204-7.

Rychli K, Huber K, Wojta J (Nov 2009). "Pigment epithelium-derived factor (PEDF) as a therapeutic target in cardiovascular disease". Expert Opinion on Therapeutic Targets. 13 (11): 1295–302.

Saha S1, Qi J, Wang S, Wang M, Li X, Kim YG, Núñez G, Gupta D, Dziarski R. "PGLYRP-2 and Nod2 are both required for peptidoglycan-induced arthritis and local inflammation." Cell Host Microbe. 2009 Feb 19;5(2):137-50

Salati S, Zini R, Bianchi E, et al. Role of CD34 antigen in myeloid differentiation of human hematopoietic progenitor cells. Stem Cells 2008;26(4):950-959.

Santucci R.A., Joyce G.F., Wise M. Male urethral stricture disease. J Urol. 2007;177:1667–1674.

Sappino AE Schiirch W, Gabbiani G. Biology of disease: differentiation repertoire of fibroblastic cells: expression of cytoskeletal proteins as marker of phenotypic modulations. Lab Invest 1990; 63: 144-61

Sceberras V, Attico E, Bianchi E, Galaverni G, Melonari M, Corradini F, Fantacci M, Ribbene A, Losi L, Balò S, Lazzeri M, Trombetta C, Rizzo M, Manfredini R, Barbagli G, Pellegrini G "Preclinical study for treatment of hypospadias by advanced therapy medicinal products". World J Urol. 2019 Jul 9.

Schmitz JC, Protiva P, Gattu AK, Utsumi T, Iwakiri Y, Neto AG, Quinn M, Cornwell ML, Fitchev P, Lugea A, Crawford SE, Chung C. "Pigment epithelium-derived factor regulates early pancreatic fibrotic responses and suppresses the profibrotic cytokine thrombospondin-1." Am J Pathol. 2011 Dec;179(6):2990-9

Sciarra A, Salciccia S, Albanesi L, Cardi A, D'Eramo G, Di Silverio F (2005) Use of cyclooxygenase-2 inhibitor for prevention of urethral strictures secondary to transurethral resection of the prostate. Urology 66(6):1218–1222

Senoo M, Pinto F, Crum CP, McKeon F. p63 Is essential for the proliferative potential of stem cells in stratified epithelia. Cell 2007; 129(3): 523-36.

Seo IY, Kim JS, Chung HT et al. Application of Antisense TGF-b Oligodeoxynucleotides on Injured Urethrae Prevents Urethral Stricture in Rats. American Urological Association, Annual Convention, 1996

Sese N, Cole M, Tawil B. Proliferation Of human keratinocytes and cocultured human keratinocytes and fibroblasts in three-dimensional fibrin constructs. Tissue Eng Part A 2011 Feb; 17(3-4):429-37

Sheikh BN, Downer NL, Phipson B, Vanyai HK, Kueh AJ, McCarthy DJ, Smyth GK, Thomas T, Voss AK (2015) MOZ and BMI1 play opposing roles during Hox gene activation in ES cells and in body segment identity specification in vivo. Proc Natl Acad Sci USA 112(17):5437–5442

Smalling RL1, Delker DA, Zhang Y, Nieto N, McGuiness MS, Liu S, Friedman SL, Hagedorn CH, Wang L. "Genome-wide transcriptome analysis identifies novel gene signatures implicated in human chronic liver disease." Am J Physiol Gastrointest Liver Physiol. 2013 Sep 1;305(5):G364-74

Snodgrass WT. Snodgrass technique for hypospadias repair. BJU Int. 2005 Mar;95(4):683-93.

Sojka DK, Plougastel-Douglas B, Yang L, Pak-Wittel MA, Artyomov MN, Ivanova Y, Zhong C, Chase JM, Rothman PB, Yu J, Riley JK, Zhu J, Tian Z, Yokoyama WM (January 2014). "Tissue-resident natural killer (NK) cells are cell lineages distinct from thymic and conventional splenic NK cells". eLife. 3: e01659.

Srinivasan M1, Bharali DJ1, Sudha T1, Khedr M1,2, Guest I3, Sell S3, Glinsky GV4, Mousa SA1. "Downregulation of Bmi1 in breast cancer stem cells suppresses tumor growth and proliferation." Oncotarget. 2017 Jun 13;8(24):38731-38742.

Sun TT (2006) Altered phenotype of cultured urothelial and other stratified epithelial cells: implications for wound healing. Am J Physiol Renal Physiol 291(1):F9–F21

Tang SH, Hammer CC, Doumanian L, Santucci RA. Adult urethral stricture disease after childhood hypospadias repair. Adv Urol 2008; 150315. Epub: Nov 4, 2008

Tian, Y., Wazir, R., Yue, X., Wang, K. J., & Li, H. (2014). Prevention of stricture recurrence following urethral endoscopic management: What do we have? Journal of Endourology, 28(5), 502–508.

Todaro, GJ; Green, H (1963). "Quantitative studies of the growth of mouse embryo cells in culture and their development into established lines". J. Cell Biol. (17): 299–313.

Tsai TH, Shih SC, Ho TC, Ma HI, Liu MY, Chen SL, Tsao YP. “Pigment epithelium-derived factor 34-mer peptide prevents liver fibrosis and hepatic stellate cell activation through down-regulation of the PDGF receptor.” PLoS One. 2014 Apr 24;9(4):e95443

Uemura, S., Hutson, J. M., Woodward, A. A., Kelly, J. H. & Chow, C. W. Balanitis xerotica obliterans with urethral stricture after hypospadias repair. Pediatr. Surg. Int. 16, 144–145 (2000)

van der Zanden LFM, van Rooij IALM, Feitz WFJ, Franke B, Knoers NVAM, Roeleveld N. Aetiology of hypospadias: a systematic review of genes and environment. Hum Reprod Update 2012;18:260e83.

Waxman SW, Morey AF (2006) Management of urethral strictures. Lancet 367 (9520): 1379–1380

Wietecha MS, Król MJ, Michalczyk ER, Chen L, Gettins PG, DiPietro LA. “Pigment epithelium-derived factor as a multifunctional regulator of wound healing.” Am J Physiol Heart Circ Physiol. 2015 Sep;309(5):H812-26

Woroniecki RP, Shatat IF, Supe K, Du Z, Kaskel FJ.Urinary cytokines and steroid responsiveness in idiopathic nephrotic syndrome of childhood. Am J Nephrol. 2008;28(1):83-90

Xue M, Jackson CJ. Extracellular Matrix Reorganization During Wound Healing and Its Impact on Abnormal Scarring. Adv Wound Care (New Rochelle). 2015 Mar 1;4(3):119-136.

Yang A, Schweitzer R, Sun D, et al. p63 is essential for regenerative proliferation in limb, craniofacial and epithelial development. Nature 1999; 398(6729): 714-8.

Yarington CT Jr. Reconstruction of the base of the tongue and lateral pharyngeal wall. Laryngoscope. 1980 Feb; 90 (2): 202-6.

Yurchenco PD, Patton BL (2009). "Developmental and pathogenic mechanisms of basement membrane assembly". Curr. Pharm. Des. 15 (12): 1277–94

Zheng GH1, Wang YJ1, Wen X1, Han XR1, Shen M1, Wang S1, Zhuang J1,2,3, Zhang ZF1, Wang L1, Hu B1, Sun CH1, Mao XY4, Yi LN4, Wu DM1, Lu J1, Zheng YL1. “Silencing of SOCS-1 and SOCS-3 suppresses renal interstitial fibrosis by alleviating renal tubular damage in a rat model of hydronephrosis.” J Cell Biochem. 2018 Feb;119(2):2200-2211

Zhong-Chu L, Yu-Hen Z, Ya-Xiong S, Yu-Feng C. One-stage Urethroplasty for hypospadias using a tube constructed with bladder mucosa – a new procedure. Urol Clin North Am. 1981 Oct; 8(3):463-70.

SUPPLEMENTARY MATERIALS

1. Supplementary protocols

S1.1. Extract of the "Clinical Protocol for Urine Collection" given to patients and healthy donors (translated from Italian).

<<Urine collection must take place according to the following indications:

- Wash your hands.
- Perform proper external genitalia and perineal zone (penis extremity) hygiene employing water and soap, wash, and dry in order not to accidentally collect external microorganisms together with the sample.
- Open the sterile cup avoiding intern's and closing cap touching.
- Proceed with urinary voiding (retracting preputial skin), paying attention not to collect first stream urine.
- Once the mid-stream is collected, close the cup.
- If the cup is wet, proceed with cleaning it.
- Wash your hands.
- Keep the sample at a temperature of 4°C and give it to the operator once in the lab/hospital.>>

2. Supplementary figures

S2.1. Heatmap of stenotic hypospadias patients (pool 2) compared to control (pool 5-5bis). Upregulated proteins are listed as red-shading blocks, whereas downregulated proteins are green-shades.

S2.2. Heatmap of stenotic non-hypospadias patients (pool 3-A) compared to control (pool 5-5bis). Upregulated proteins are listed as red-shading blocks, whereas downregulated proteins are green-shades.

S2.3. Heatmap of stenotic hypospadias patients (pool 2) compared to non-hypospadias patients (pool 3-A). Upregulated proteins are listed as red-shading blocks, whereas downregulated proteins are green-shades.

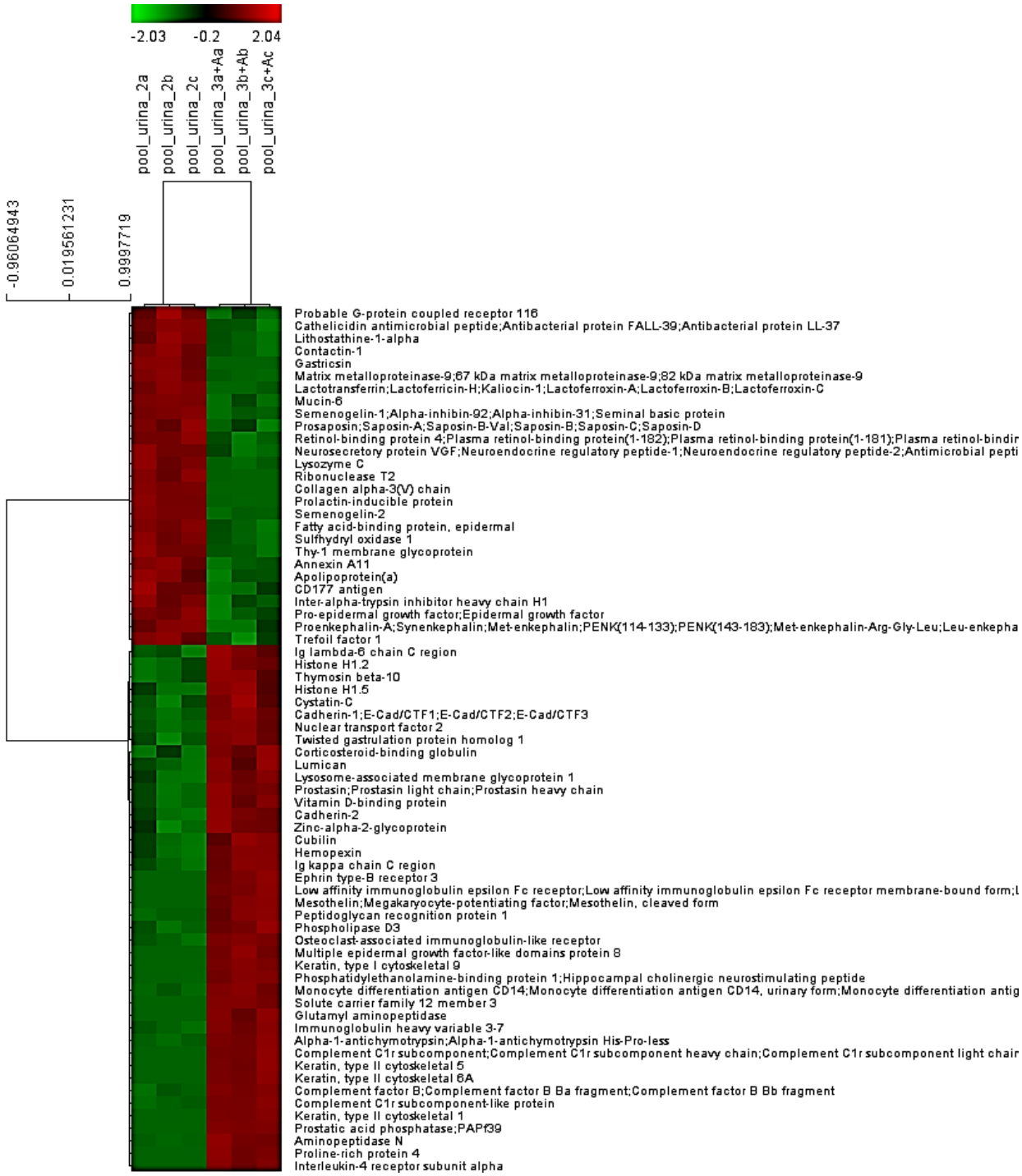

3. Supplementary tables

S3.1. Differentially expressed proteins in urethral stricture patients with hypospadias; fold-changes are indicated in relation to the control group.

UniProt ID	Protein name	p-value	Fold change
P68104	Elongation factor 1-alpha 1	4.96E-03	undetected in CTRL
P05164	Myeloperoxidase	7.31E-04	20.37115364
P61626	Lysozyme C	6.27E-06	5.278019587
Q02383	Semenogelin-2	7.91E-04	5.210672055
P04279	Semenogelin-1	2.71E-04	4.358090186
P12273	Prolactin-inducible protein	1.18E-04	3.062909638
P15311	Ezrin	8.38E-04	2.823374973
P49913	Cathelicidin antimicrobial peptide	2.05E-03	2.823159833
P80188	Neutrophil gelatinase-associated lipocalin	3.24E-05	2.752409415
P04083	Annexin A1;Annexin	2.02E-03	2.676304418
Q6W4X9	Mucin-6	7.70E-05	2.674790583
P53990	IST1 homolog	2.27E-03	2.49700113
Q96DA0	Zymogen granule protein 16 homolog B	5.18E-04	2.31716359
Q96MG2	Junctional sarcoplasmic reticulum protein 1	1.18E-03	2.148722206
Q96FE7	Phosphoinositide-3-kinase-interacting protein 1	2.72E-03	2.114342506
P08138	Tumor necrosis factor receptor superfamily member 16	3.65E-03	2.056653606
Q08380	Galectin-3-binding protein	3.17E-03	-2.022497845
P08582	Melanotransferrin	3.23E-04	-2.048917162
Q8IWY4	Signal peptide, CUB and EGF-like domain-containing protein 1	2.06E-03	-2.059738321
P05156	Complement factor I	1.48E-04	-2.068623006
O14773	Tripeptidyl-peptidase 1	1.71E-03	-2.092736198
A0A087WV17	Osteoclast-associated immunoglobulin-like receptor	7.43E-04	-2.10187952
P14543	Nidogen-1	1.19E-03	-2.103475473
P01033	Metalloproteinase inhibitor 1	3.89E-03	-2.110842548
P08473	Neprilysin	2.42E-04	-2.166770785
Q969H8	Myeloid-derived growth factor	2.96E-03	-2.324330296
O43405	Cochlin	3.62E-05	-2.375165349
Q6UVK1	Chondroitin sulfate proteoglycan 4	1.90E-04	-2.418361867
P54760	Receptor protein-tyrosine kinase	9.12E-04	-2.456823436
Q8WVQ1	Soluble calcium-activated nucleotidase 1	1.20E-03	-2.485740451
P05543	Thyroxine-binding globulin	4.64E-04	-2.498087149
P04180	Phosphatidylcholine-sterol acyltransferase	2.13E-03	-2.500755523
P30086	Phosphatidylethanolamine-binding protein 1	6.83E-04	-2.583275079
P02765	Alpha-2-HS-glycoprotein	4.43E-05	-2.587583205
Q96S96	Phosphatidylethanolamine-binding protein 4	1.77E-03	-2.639654611
P11717	Cation-independent mannose-6-phosphate receptor	2.22E-03	-2.741832235
O00187	Mannan-binding lectin serine protease 2	1.70E-03	-2.742146954
O75594	Peptidoglycan recognition protein 1	7.50E-05	-2.85305759
O75503	Ceroid-lipofuscinosis neuronal protein 5	1.36E-03	-3.13372061
P01834	Ig kappa chain C region	1.83E-03	-3.408364719
Q16661	Guanylate cyclase activator 2B	2.65E-04	-3.491006845
P05154	Plasma serine protease inhibitor	5.61E-05	-4.062941728
Q8IV08	Phospholipase D3	1.69E-03	-4.178470448
P15144	Aminopeptidase N	1.12E-03	-4.191449319
P16444	Dipeptidase 1	9.38E-05	-4.557920491
P08185	Corticosteroid-binding globulin	1.14E-04	-4.577674835
P08118	Beta-microseminoprotein	2.90E-04	-4.679611184

UniProt ID	Protein name	p-value	Fold change
P08571	Monocyte differentiation antigen CD14	1.93E-05	-5.149473076
P61769	Beta-2-microglobulin	2.80E-05	-6.015163567
P01011	Alpha-1-antichymotrypsin	6.93E-04	-6.24683427
P07737	Profilin-1	3.05E-03	-6.425228119
Q96PD5	N-acetylmuramoyl-L-alanine amidase	1.51E-03	-7.242308933
P07288	Prostate-specific antigen	9.37E-04	-7.909849388
P05090	Apolipoprotein D	1.65E-05	-8.014327027
P04264	Keratin, type II cytoskeletal 1	6.37E-04	-8.514397231
P15309	Prostatic acid phosphatase	7.47E-04	-9.988339192
P61970	Nuclear transport factor 2	1.32E-03	-15.50927971
P13645	Keratin, type I cytoskeletal 10	4.31E-04	-28.34244405
P02750	Leucine-rich alpha-2-glycoprotein	8.72E-04	-91.72504725
Q14019	Coactosin-like protein	1.93E-05	undetected in patients
O15197	Ephrin type-B receptor 6	3.98E-05	undetected in patients
P04433	Ig kappa chain V-III region VG	8.84E-05	undetected in patients
Q9BQ51	Programmed cell death 1 ligand 2	1.71E-04	undetected in patients
P17050	Alpha-N-acetylgalactosaminidase	2.74E-04	undetected in patients
P17931	Galectin-3	3.51E-04	undetected in patients
Q6P531	Gamma-glutamyltransferase 6	4.43E-04	undetected in patients
P36955	Pigment epithelium-derived factor	4.79E-04	undetected in patients
P01019	Angiotensinogen	5.97E-04	undetected in patients
O43155	Leucine-rich repeat transmembrane protein FLRT2	6.24E-04	undetected in patients
Q8NCC3	Group XV phospholipase A2	7.13E-04	undetected in patients
P29508	Serpin B3	7.97E-04	undetected in patients
Q12794	Hyaluronidase-1	8.71E-04	undetected in patients
P12872	Promotilin	1.11E-03	undetected in patients
Q15485	Ficolin-2	1.16E-03	undetected in patients
P29622	Kallistatin	1.33E-03	undetected in patients
Q99538	Legumain	1.53E-03	undetected in patients
P20138	Myeloid cell surface antigen CD33	1.55E-03	undetected in patients
P09211	Glutathione S-transferase P	1.71E-03	undetected in patients
P00746	Complement factor D	1.73E-03	undetected in patients
Q03154	Aminoacylase-1	1.78E-03	undetected in patients
P34059	N-acetylgalactosamine-6-sulfatase	1.91E-03	undetected in patients
O00499	Myc box-dependent-interacting protein 1	2.02E-03	undetected in patients
P06733	Alpha-enolase	2.14E-03	undetected in patients
Q8IZA0	Dyslexia-associated protein KIAA0319-like protein	2.14E-03	undetected in patients
Q9BQT9	Calsyntenin-3	2.27E-03	undetected in patients
P04406	Glyceraldehyde-3-phosphate dehydrogenase	2.86E-03	undetected in patients
Q9BRK3	Matrix-remodeling-associated protein 8	2.98E-03	undetected in patients
Q13508	Ecto-ADP-ribosyltransferase 3	3.03E-03	undetected in patients
Q93088	Betaine-homocysteine S-methyltransferase 1	3.14E-03	undetected in patients
P04066	Tissue alpha-L-fucosidase	3.32E-03	undetected in patients
P35527	Keratin, type I cytoskeletal 9	3.49E-03	undetected in patients
Q08345	Epithelial discoidin domain-containing receptor 1	3.58E-03	undetected in patients
P06734	Low affinity immunoglobulin epsilon Fc receptor	3.87E-03	undetected in patients
Q8N4F0	BPI fold-containing family B member 2	3.90E-03	undetected in patients
P54289	Voltage-dependent calcium channel subunit alpha-2/delta-1	3.97E-03	undetected in patients
P48061	Stromal cell-derived factor 1	4.19E-03	undetected in patients
P12821	Angiotensin-converting enzyme	4.35E-03	undetected in patients
Q9NQ79	Cartilage acidic protein 1	4.64E-03	undetected in patients
P41271	Neuroblastoma suppressor of tumorigenicity 1	4.70E-03	undetected in patients
P09467	Fructose-1,6-bisphosphatase 1	4.85E-03	undetected in patients

***S3.1** continued*

S3.2. Differentially expressed proteins in urethral stricture patients without hypospadias; fold-changes are indicated in relation to the control group.

UniProt ID	Protein name	p-value	Fold change
P32320	Cytidine deaminase	2.20E-03	undetected in CTRL
Q6ISS4	Leukocyte-associated immunoglobulin-like receptor 2	3.23E-03	undetected in CTRL
P35527	Keratin, type I cytoskeletal 9	3.52E-03	17.03318089
P63313	Thymosin beta-10	2.66E-04	14.45992338
P13647	Keratin, type II cytoskeletal 5	1.40E-03	12.86680929
P04264	Keratin, type II cytoskeletal 1	1.08E-04	5.388820776
P13796	Plastin-2	2.12E-03	4.502175393
P13645	Keratin, type I cytoskeletal 10	3.69E-03	3.761633234
P80297	Metallothionein-1X	3.82E-03	3.371287188
P16401	Histone H1.5	1.39E-03	3.102581329
Q8IWU5	Extracellular sulfatase Sulf-2	1.47E-03	2.844430675
P59666	Neutrophil defensin 3	1.78E-03	2.620239427
Q9Y6R7	IgGFc-binding protein	5.12E-05	2.537226978
P01780	Ig heavy chain V-III region JON	3.08E-03	2.534940821
Q9UKY0	Prion-like protein doppel	4.46E-03	2.217756017
P06454	Prothymosin alpha	1.45E-03	2.174290799
P16070	CD44 antigen	4.37E-03	2.164181771
P80188	Neutrophil gelatinase-associated lipocalin	1.44E-04	2.117713875
P22352	Glutathione peroxidase 3	1.36E-03	-2.140122892
P06396	Gelsolin	1.94E-04	-2.200853992
P02765	Alpha-2-HS-glycoprotein	1.36E-03	-2.274083282
P08571	Monocyte differentiation antigen CD14	1.02E-04	-2.312179251
P00734	Prothrombin	3.98E-03	-2.321463878
P19827	Inter-alpha-trypsin inhibitor heavy chain H1	3.85E-03	-2.411630695
P02814	Submaxillary gland androgen-regulated protein 3B	1.55E-03	-2.503586861
P05090	Apolipoprotein D	1.41E-04	-2.511656338
Q8IWA5	Choline transporter-like protein 2	4.68E-03	-2.524869391
Q6UX06	Olfactomedin-4	1.83E-03	-2.602771482
P50995	Annexin A11	1.36E-03	-2.607793714
Q96PD5	N-acetylmuramoyl-L-alanine amidase	3.34E-03	-2.660395
P14543	Nidogen-1	1.47E-03	-2.717382151
P05154	Plasma serine protease inhibitor	1.13E-03	-3.02472471
Q92692	Nectin-2	1.26E-03	-3.233844764
P0C0L5	Complement C4-B	1.71E-04	-3.642956572
P61970	Nuclear transport factor 2	1.65E-03	-3.766187587
P07288	Prostate-specific antigen	2.01E-03	-4.769755787
Q12907	Vesicular integral-membrane protein VIP36	3.07E-04	-4.8386281
Q16661	Guanylate cyclase activator 2B	2.55E-03	-5.140565763

UniProt ID	Protein name	p-value	Fold change
P08118	Beta-microseminoprotein	1.28E-03	-5.230539068
P61769	Beta-2-microglobulin	1.23E-03	-6.601291856
Q08629	Testican-1	4.97E-03	-9.706479163
Q6NUS6	Tectonic-3	8.16E-05	undetected in patients
P12429	Annexin A3	1.87E-04	undetected in patients
P04433	Ig kappa chain V-III region VG	2.01E-04	undetected in patients
P17931	Galectin-3	3.41E-04	undetected in patients
O43155	Leucine-rich repeat transmembrane protein FLRT2	6.16E-04	undetected in patients
P12821	Angiotensin-converting enzyme	9.23E-04	undetected in patients
Q86TH1	ADAMTS-like protein 2	9.83E-04	undetected in patients
P29508	Serpin B3	1.26E-03	undetected in patients
P29622	Kallistatin	1.31E-03	undetected in patients
P12872	Promotilin	1.36E-03	undetected in patients
P00746	Complement factor D	1.71E-03	undetected in patients
P30046	D-dopachrome decarboxylase	2.19E-03	undetected in patients
Q9UN70	Protocadherin gamma-C3	2.23E-03	undetected in patients
Q9NQ79	Cartilage acidic protein 1	2.29E-03	undetected in patients
Q8N126	Cell adhesion molecule 3	2.46E-03	undetected in patients
Q8TF66	Leucine-rich repeat-containing protein 15	2.49E-03	undetected in patients
P10912	Growth hormone receptor	2.56E-03	undetected in patients
P04406	Glyceraldehyde-3-phosphate dehydrogenase	2.85E-03	undetected in patients
P36955	Pigment epithelium-derived factor	2.94E-03	undetected in patients
P63104	14-3-3 protein zeta/delta	2.97E-03	undetected in patients
Q9BRK3	Matrix-remodeling-associated protein 8	2.99E-03	undetected in patients
Q93088	Betaine-homocysteine S-methyltransferase 1	3.11E-03	undetected in patients
Q8N4F0	BPI fold-containing family B member 2	3.87E-03	undetected in patients
Q86T13	C-type lectin domain family 14 member A	3.88E-03	undetected in patients
Q9H336	Cysteine-rich secretory protein LCCL domain-containing 1	4.01E-03	undetected in patients
Q96JQ0	Protocadherin-16	4.63E-03	undetected in patients
P36980	Complement factor H-related protein 2	4.70E-03	undetected in patients
P23528	Cofilin-1	4.78E-03	undetected in patients

S3.2 *continued*

S3.3. Differentially expressed proteins in urethral stricture patients with hypospadias compared to patients without hypospadias; proteins that were not significantly different with the control group are not displayed.

UniProt ID	Protein name	p-value	Fold change
P61626	Lysozyme C	3.79E-03	5.768565
Q02383	Semenogelin-2	5.67E-05	3.480283
P04279	Semenogelin-1	1.03E-04	3.438502
P50995	Annexin A11	7.81E-04	2.907207
P12273	Prolactin-inducible protein	1.24E-03	2.554697
Q6W4X9	Mucin-6	3.03E-03	2.407703
P19827	Inter-alpha-trypsin inhibitor heavy chain H1	1.70E-03	2.279761
P01834	Ig kappa chain C region	8.97E-04	-2.10368
P16401	Histone H1.5	4.32E-03	-2.21459
P08571	Monocyte differentiation antigen CD14	1.88E-04	-2.57272
Q8IYS5	Osteoclast-associated immunoglobulin-like receptor	1.26E-03	-2.60112
P63313	Thymosin beta-10	3.00E-03	-3.17923
O75594	Peptidoglycan recognition protein 1	4.23E-03	-3.56353
P15144	Aminopeptidase N	2.19E-03	-3.76409
P01011	Alpha-1-antichymotrypsin	1.78E-03	-3.81068
P30086	Phosphatidylethanolamine-binding protein 1	9.51E-04	-3.89319
P61970	Nuclear transport factor 2	6.53E-04	-4.54847
P15309	Prostatic acid phosphatase	8.06E-05	-11.6672
P04264	Keratin, type II cytoskeletal 1	2.74E-04	-163.803
P35527	Keratin, type I cytoskeletal 9	6.22E-04	undetected in patients
Q8IV08	Phospholipase D3	1.04E-03	undetected in patients
P06734	Low affinity immunoglobulin epsilon Fc receptor	1.74E-03	undetected in patients
P13647	Keratin, type II cytoskeletal 5	2.52E-03	undetected in patients

S3.4. Gene Ontology (GO) terms of biological processes, cellular compartments, and molecular functions investigated in hypospadias and non-hypospadias urethral stricture patients.

Category	Term	Category	Term
Biological process (BP)		GO:0050830	Defense response to Gram-positive bacterium
GO:0000302	Response to reactive oxygen species	GO:0071222	Cellular response to lipopolysaccharide
GO:0001525	Angiogenesis	GO:0071493	Cellular response to UV-B
GO:0001822	Kidney development	GO:0071638	Monocyte chemotactic protein-1 production negative regulation
GO:0001867	Complement activation, lectin pathway	GO:0071711	Basement membrane organization
GO:0001895	Retina homeostasis	GO:1900005	Serine-type endopeptidase activity positive regulation
GO:0002003	Angiotensin maturation	GO:1900121	Negative regulation of receptor binding
GO:0002019	Renal output regulation by angiotensin	GO:1901318	Sperm motility negative regulation
GO:0002221	Pattern recognition receptor signaling pathway	Cellular component (CC)	
GO:0002576	Platelet degranulation	GO:0005576	Extracellular region
GO:0003014	Renal system process	GO:0005615	Extracellular space
GO:0003081	Systemic arterial blood pressure regulation by renin-angiotensin	GO:0005764	Lysosome
GO:0006094	Gluconeogenesis	GO:0005768	Endosome
GO:0006508	Proteolysis	GO:0005886	Plasma membrane
GO:0006749	Glutathione metabolic process	GO:0005925	Focal adhesion
GO:0006898	Receptor-mediated endocytosis	GO:0009897	External side of plasma membrane
GO:0006909	Phagocytosis	GO:0009986	Cell Surface
GO:0006954	Inflammatory response	GO:0016020	Membrane
GO:0006955	Immune response	GO:0016528	Sarcoplasm
GO:0006956	Complement activation	GO:0031012	Extracellular matrix
GO:0006958	Complement activation, classical pathway	GO:0031093	Platelet Alpha Granule Lumen
GO:0007156	Homophilic cell adhesion via plasma membrane adhesion molecules	GO:0031982	Vesicle
GO:0007157	Heterophilic cell-cell adhesion via plasma membrane cell adhesion molecules	GO:0042581	Specific granule
GO:0007568	Aging	GO:0042582	Azurophil granule
GO:0009253	Peptidoglycan catabolic process	GO:0043202	Lysosomal Lumen
GO:0009615	Response to virus	GO:0070062	Extracellular exosome
GO:0010951	Negative regulation of endopeptidase activity	GO:0072562	Blood microparticle
GO:0016139	Glycoside catabolic process	Molecular function (MF)	
GO:0016525	Angiogenesis negative regulation	GO:0001948	Glycoprotein binding
GO:0019731	Antibacterial humoral response	GO:0002020	Protease binding
GO:0022617	Extracellular matrix disassembly	GO:0004175	Endopeptidase activity
GO:0030308	Cell growth negative regulation	GO:0004252	Serine-type endopeptidase activity
GO:0031100	Organ regeneration	GO:0004867	Serine-type endopeptidase inhibitor activity
GO:0032092	Protein binding positive regulation	GO:0004869	Cysteine-type endopeptidase inhibitor activity
GO:0032689	Interferon-gamma production negative regulation	GO:0004872	Receptor activity
GO:0032827	Natural killer cell differentiation involved in immune response negative regulation	GO:0005509	Calcium ion binding
GO:0032836	Glomerular basement membrane development	GO:0005518	Collagen binding
GO:0032930	Superoxide anion generation positive regulation	GO:0008233	Peptidase activity
GO:0042742	Defense response to bacterium	GO:0008236	Serine-type peptidase activity
GO:0042989	Sequestering of actin monomers	GO:0008237	Metallopeptidase activity
GO:0043066	Apoptotic process negative regulation	GO:0008238	Exopeptidase activity
GO:0043171	Peptide catabolic process	GO:0008240	Tripeptidyl-peptidase activity
GO:0043434	Response to peptide hormone	GO:0008745	N-acetylmuramoyl-L-alanine amidase activity
GO:0044117	Symbiont growth in host	GO:0016019	Peptidoglycan receptor activity
GO:0044267	Cellular protein metabolic process	GO:0019863	IgE binding
GO:0045087	Innate immune response	GO:0030246	Carbohydrate binding
GO:0045766	Angiogenesis positive regulation	GO:0036094	Small molecule binding
GO:0050663	Cytokine secretion	GO:0042277	Peptide binding
GO:0050727	Inflammatory response regulation	GO:0043236	Laminin binding
GO:0050776	Regulation of immune response	GO:0048306	Calcium-dependent protein binding
GO:0050817	Coagulation	GO:0070573	Metallodipeptidase activity
GO:0050829	Defense response to Gram-negative bacterium		